Adaptive Dynamic Inversion Control of Linear Plants With Control Position Constraints

John Valasek, *Senior Member, IEEE*, Maruthi Ram Akella, *Member, IEEE*, Anshu Siddarth, *Student Member, IEEE*, and Elizabeth Rollins, *Student Member, IEEE*

***Abstract*—For a class of linear time-invariant systems with uncertain parameters, this paper proposes and develops a notion of the Domain of Control Authority to achieve stable adaptation in the presence of control position limits. The Domain of Control Authority defines the subspace in which the plant state can be driven in any arbitrary direction by bounded control. No restrictions are placed on the stability of the open-loop system. To address the problem of containing the state within the Domain of Control Authority, a switching control strategy with a direction consistent control constraint mechanism is developed for an unstable plant. This restricts the resultant direction of the rate of change of the state to be the same as the direction of the desired reference state. Stability proofs are provided, and controller performance is demonstrated with numerical examples of a two degree-of-freedom dynamic model and an F-16XL aircraft model.**

***Index Terms*—Adaptive control, control saturation constraints, direction consistent control constraint mechanism, dynamic inversion, linear systems.**

I. Introduction

ACTUATOR saturation is a major consideration for all practical control systems, and many strategies to overcome its effects have been studied. For example, Hu and Lin have done seminal work in analyzing the controllability and stabilization of unstable, linear time-invariant systems with input saturation [1]–[3]. They explicitly identified the null controllable region of the state-space for linear systems with saturated linear feedback. However, their work does not address systems with uncertain parameters. Traditionally, adaptive control assumes full control authority and lacks a theoretical basis for control in the presence of actuator saturation limits. Saturation is a problem for adaptive systems since continued adaptation in the presence of saturation may lead to instability. In the past, much effort has been expended for adaptive control design in the presence of input saturation constraints [4]. Karason and Annaswamy presented the concept of modifying the error proportional to the control deficiency [5]. They laid out a rigorous mathematical proof of the boundedness of signals for a model reference framework and identified a set of initial conditions of the plant and the controller for which a stable controller could be realized. Akella, Junkins, and Robinett devised a methodology to impose actuator saturation constraints on the adaptive control law analogous to Pontryagin's principle for optimal control in order to make the error energy rate as negative as possible with admissible controls [6]. They identified a boundary layer term, which is the difference between the calculated control and the applied control, and imposed conditions on the adaptive update laws to bound the boundary layer thickness. More recently, Johnson and Calise applied the concept of "pseudo-control hedging" to adaptive control, which is a fixed gain adjustment to the reference model that is proportional to the control deficiency [7]. Lavretsky and Hovakimyan have proposed a new design approach called "positive μ-modification" that guarantees that the control never incurs saturation [8]. In [9] the "$\mathcal{L}_1$ adaptive controller" is extended to include control constraints for linear plants with known control influence. Hong and Yao [10] synthesized a robust controller specifically for precision control of linear motor drive systems using backstepping, while addressing the different physical uncertainties. Kahveci and Ioannou [11] extended the anti-windup compensator design for stable systems with actuator position and rate limits, and a similar problem was addressed in Leonessa *et al.* [12] by modifying the reference to maintain system stability and control within bounds.

Dynamic Inversion is an approach which has been widely used in recent years for the control of nonlinear systems, especially in the field of aerospace engineering [13]–[16]. A fundamental assumption in this approach is that the inherent plant dynamics are modeled accurately, and therefore can be canceled exactly by the feedback functions. In practice, this assumption is not realistic; the dynamic inversion controller requires some level of robustness to suppress undesired behavior due to plant uncertainties. To overcome this robustness problem, an adaptive model of the plant dynamics sometimes is used to facilitate the inversion, which is then updated in real-time based on the response of the system. This gives rise to an entire class of controllers which may be referred to as adaptive dynamic inversion controllers [17].

This paper investigates problems introduced in adaptive dynamic inversion control schemes due to bounds on the control

Manuscript received October 21, 2010; revised February 03, 2011; accepted June 11, 2011. Manuscript received in final form June 13, 2011. Date of publication July 25, 2011; date of current version May 22, 2012. Recommended by Associate Editor N. Hovakimyan. This work was supported in part by the U.S. Air Force Office of Scientific Research under Contract FA9550–08-1–0038, with technical monitor Dr. F. Fahroo, and by the Texas Institute for Intelligent Bio-Nano Materials and Structures. Any opinions, findings, and conclusions or recommendations expressed in this material are those of the author(s) and do not necessarily reflect the views of the U.S. Air Force or NASA.

J. Valasek, A. Siddarth and E. Rollins are with the Vehicle Systems and Controls Laboratory, Aerospace Engineering Department, Texas A&M University, College Station, TX 77843-3141 USA (e-mail: valasek@tamu.edu; anshun1@tamu.edu; erollins@tamu.edu).

M. R. Akella is with the Department of Aerospace Engineering and Engineering Mechanics, University of Texas at Austin, Austin, TX 78712-0235 USA (e-mail: makella@mail.utexas.edu).

Color versions of one or more of the figures in this paper are available online at http://ieeexplore.ieee.org.

Digital Object Identifier 10.1109/TCST.2011.2159976

and develops a three component control scheme to overcome them. The contributions of this paper are the identification of the domain of attraction considering the control position limit and the development of a switching control strategy to contain the plant within this domain. Another novel idea is that of a direction consistent control constraint mechanism in the presence of control saturation. This is achieved in part by preserving the control input direction. While the idea of preserving the control input direction using control allocation is not entirely new [18], it is restricted to preserving the direction of the control vector only. This paper formalizes and extends a concept by Tandale and Valasek in [19] that not only preserves the direction of the control, but also attempts to preserve the direction of the resultant rate of change of the state to be the same as that of the desired rate. Additionally, a modified adaptation mechanism is implemented to prevent incorrect adaptation arising from trajectory errors due to control saturation. Here the mathematical development of the control scheme and the adaptation mechanisms is presented, along with proofs for the convergence of the tracking error and the stability of the overall control scheme.

This paper is organized as follows. Section II describes the class of plants that are considered. Section III defines the concept of the Domain of Control Authority (DCA) for plants with bounded control. The switching control strategy and the direction consistent control constraint mechanism are explained in Section IV. The development of the control law and the modified update law to prevent the incorrect update of parameters due to saturation is presented in Section VI. Section VII presents simulation results for a two-dimensional planar plant and an F-16XL aircraft model. Finally, conclusions are presented in Section VIII.

II. System Dynamics

Consider linear time-invariant continuous dynamic systems of the form

$$\dot{\mathbf{x}} = A\mathbf{x} + B\mathbf{u}_a \tag{1}$$

where $\mathbf{x}(t) \in \mathbb{R}^n$ is the state vector, $A \in \mathbb{R}^{n\times n}$ is the matrix of unknown plant parameters, $\mathbf{u}_a(t) \in \mathbb{R}^n$ is the vector of applied controls driving the system, and $B \in \mathbb{R}^{n\times n}$ is the unknown control effectiveness matrix. For this work, the number of controls equals the number of states so that the control effectiveness matrix is square and non-singular to permit dynamic inversion. Each control u_{a_i} is symmetrically bounded between the values $[-u_{m_i}, +u_{m_i}]$. The plant matrices A and B are not known exactly. The nominal values of the plant matrices $\bar{A}$ and $\bar{B}$ are specified, with a percentage uncertainty for each element of the plant matrix given as

$$A_{ij} = \bar{A}_{ij} + \triangle A_{ij} \tag{2}$$

$$B_{ij} = \bar{B}_{ij} + \triangle B_{ij} \tag{3}$$

where $|\triangle A_{ij}| \leq 0.05|\bar{A}_{ij}|$ and $|\triangle B_{ij}| \leq 0.05|\bar{B}_{ij}|$.

The reference trajectory is specified in terms of $\mathbf{x}_r$, which is chosen such that it is uniformly continuous, bounded, and differentiable with first order continuous, bounded derivatives $\dot{\mathbf{x}}_r$. The control objective is to track any feasible reference trajectory that can be followed within the control limits. For trajectories that are not feasible with respect to the control limits, the objective is to track the reference trajectory as closely as possible, while maintaining stability and ensuring that all signals remain bounded. Further, it is assumed that the entire state vector is measurable and that no observer is necessary to estimate the states.

III. Domain of Control Authority (DCA)

One of the most fundamental issues associated with the control of a system is controllability. While unconstrained controllability [20] has been well understood for several decades, the understanding of constrained controllability is incomplete [4]. The following discussion considers how bounds on controls affect controllability. While a linear scalar plant is used to elucidate the concepts, the discussion extends to multiple-input-multiple-output (MIMO) plants in which the number of controls equals the number of states. Consider

$$\dot{x} = -a^*x + b^*u_a \tag{4}$$

where $x(t) \in \mathbb{R}^1$, and a^*, b^* are unknown scalars with $b^* \neq 0$ and $a^* > 0$ such that the inherent dynamics are stable. The applied control u_a is bounded symmetrically as $u_a \in [-u_m, +u_m]$, where $u_m > 0$ is a known control limit.

There are two types of constraints that may be imposed on the plant state-space because of the bounds on the control.

1) ***Control Authority Constraint:*** If the plant is open-loop stable, the only diverging tendency that can propagate the system away from the equilibrium point is provided by the control. This diverging tendency can be infinite for a system which is controllable and has unbounded control. If the control is bounded, there will be a boundary in the state-space beyond which the converging tendency of the plant is greater than the diverging tendency due to the bounded control.
2) ***Tracking Constraint:*** Consider the plant model from (4). Since the control is bounded within $[-u_m, +u_m]$, the rate of change of the state at any point of time is bounded by

$$\dot{x} = \begin{cases} -a^*x + b^*u_m, & \text{if } u = u_m \\ -a^*x - b^*u_m, & \text{if } u = -u_m \end{cases} \tag{5}$$

where x is the plant state at that instant of time. Any reference trajectory that the plant can successfully track must satisfy the rate bounds listed in (5).

The controllability test for linear systems ensures that the control can affect every state, but does not consider the effect of bounds on the control. To have complete authority over the plant, the bounded control must be able to overcome the inherent plant dynamics and prescribe the desired dynamics.

A. Case 1: Stable Plant ($a^* > 0$)

Considering the plant model of (4), the inherent plant dynamics are given by the term $-a^*x$. The control authority is limited by the bounds on the control to values of $\pm b^*u_m$, so there exists boundaries in the plant state-space beyond which the inherent plant dynamics will dominate the control effort, and the plant will not be controllable. These boundaries will be reached when an extremal control is necessary to cancel the inherent plant dynamics. In the interior region the control has the ability

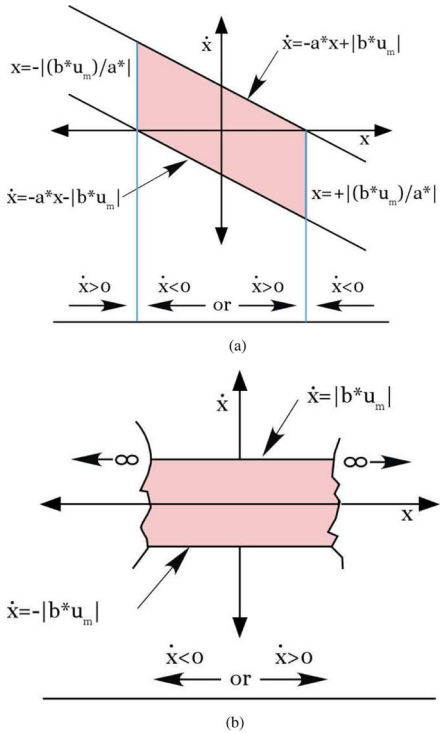

Fig. 1. Phase plot showing the domain for a traceable trajectory for an open-loop stable plant and for a neutrally stable plant. (a) Phase plot for an open-loop stable plant. (b) Phase plot for a neutrally stable plant.

to nullify the inherent plant dynamics without reaching its extremal values. This interior region is called the DCA. Referring to Fig. 1(a), the boundaries in terms of the plant state are

$$-a^* x_{\text{bound}} = -b^* u_a \tag{6}$$

$$-a^* x_{\text{bound}} = \pm b^* u_m \tag{7}$$

$$x_{\text{bound}} = \pm \frac{b^* u_m}{a^*}. \tag{8}$$

Equation (8) gives the vertical bound, and (5) gives the bounds on the rate of change of the state. Outside of the DCA boundary $\dot{x} < 0$ and the plant moves toward the origin. If the initial state is within the DCA, then the control cannot drive the state outside the DCA. If the initial state is outside the DCA, the inherent plant dynamics will drive the state into the DCA. Thus the bounded control does not lead to instability for an open-loop stable plant, but only to a limited operational envelope for the plant.

B. Case 2: Neutrally Stable Plant $(a^* = 0)$

The derivative of the state is affected only by the control

$$\dot{x} = b^* u_a. \tag{9}$$

The plant state is not bounded and can take any value on $[-\infty, +\infty]$, but the rate of change of the state is limited due to the control bound. The rate limits for a traceable trajectory [see Fig. 1(b)] are

$$|\dot{x}_r| \leq b^* u_m. \tag{10}$$

C. Case 3: Unstable Plant: $(a^* < 0)$

For current state x the unforced response $-a^* x$ drives the plant away from the state $x = 0$. If the plant reaches a state where the destabilizing tendency becomes greater than the maximum restoring contribution that the control can provide, then the state continues to diverge, such that $x \to \infty$ if $|x| > |b^* u_m / a^*|$. These points determine the boundary of the DCA. If the state crosses these points, stability of the system cannot be recovered.

IV. Switching Control Strategy

Consider a plant that is required to track an arbitrary reference trajectory using a dynamic inversion controller. The bounded control must cancel the inherent plant dynamics yet retain sufficient control effort to prescribe a rate of change of the state in any arbitrary direction of the state-space. If an extremal value of control is necessary to cancel the inherent plant dynamics, then there is at least one direction in which the plant state cannot be driven. Therefore, *the DCA consists of the set of the system equilibrium states. Depending on the system stability, some of these plant states can be driven in any arbitrary direction by a bounded control*. The boundary of the DCA is defined by the states in which at least one control must take on its extremal value in order to cancel the inherent plant dynamics. Outside the DCA open-loop stable plants can never cross the DCA boundary and remain bounded. Unstable plants diverge since the inherent diverging tendency dominates the maximum possible converging tendency that the control can provide.

The solution strategy proposed here is to identify the DCA and to develop a control law to prevent the plant state from crossing the DCA boundary. The control required to perform the tracking objective may be applied when the state is not near the DCA boundary. Once the state nears the DCA boundary, the control can be switched to a stabilizing control that cancels the plant dynamics and provides a restoring tendency toward the origin. It should be noted that whenever the state is within the DCA, the magnitude of the rate of change of the state is restricted because of the bounded control, but the direction of the rate of change of the state is not limited. The Sections IV-A and IV-B discuss methods to identify the DCA boundary and the concept of stabilizing control.

A. Enforcing the Switching Control Law Without Explicit Identification of the DCA Boundary

The DCA is defined by the states where at least one control must equal its extremal value in order to cancel the inherent plant dynamics. At the boundary of the DCA, (1) becomes

$$0 = A^* \mathbf{x}_{\text{boundary}} + B^* \mathbf{u}_{\text{extremal}}. \tag{11}$$

The entire DCA boundary can be evaluated by substituting all possible values that the vector $\mathbf{u}$ can take such that $u_i = \pm u_{m_i}$ for at least one i, where $i = 1, \ldots, n$ and u_i indicates the ith control input.

Consider a 2-D state-space for simplicity of analysis. The DCA for this 2-D state-space defines a rectangular parallelogram whose vertices are obtained from (11) when both compo-

nents of the control vector are equal to any one of the four possible permutations of the extremal values $(\pm u_{m_1}, \pm u_{m_2})$. The edges of the parallelogram correspond to cases when only one component of the control vector is equal to an extremal value. The other component of the control vector can equal any value within the control bounds. Consequently, the DCA boundary can be calculated and stored. As the state approaches the DCA boundary, the control can be switched from a tracking control to a stabilizing control. This idea easily extends to n-dimensions, where the DCA is an n-dimensional parallelepiped. However, this approach requires explicit identification and storage of the DCA boundary, which can be computationally intensive for higher dimensional plants.

An alternate approach for determining the switching control law is to use a scalar measure that keeps track of how close the operating point is to the DCA boundary, instead of defining the DCA boundary explicitly. This approach can be implemented by identifying the control component necessary to cancel the inherent plant dynamics, $\mathbf{u}_{\text{cancel}}$, which can be obtained by solving the following equation at run-time:

$$\mathbf{u}_{\text{cancel}} = -B^{*-1}A^{*}\mathbf{x}. \tag{12}$$

The applied control can be switched from tracking to stability as $\mathbf{u}_{\text{cancel}}$ approaches $\mathbf{u}_{\text{extremal}}$, which occurs when at least one component of $\mathbf{u}_{\text{cancel}}$ is equal to $\mathbf{u}_m$. Since (12) is simple to solve can be solved at every time step, this approach eliminates the need for prior explicit identification of the DCA.

B. Direction Consistent Control Constraint Mechanism

For a multi-input plant the bounded control not only restricts the magnitude of the applied control, but also changes the direction of the system. Fig. 2 illustrates this concept. Consider a scenario with two controls u_1 and u_2. Assume that the control calculated by the control algorithm to track a desired reference $\mathbf{u}_c$ is greater than the control bounds shown by the box. If each control is saturated to its respective maximum, the control applied to the plant, $\mathbf{u}_a$, has a significantly different direction compared to $\mathbf{u}_c$. When this control is applied to the plant the resulting rate of change of state also has a different direction than the desired direction. Here we develop a control strategy that implements $\mathbf{u}_a$, direction consistent shown in Fig. 2 that is within the position limits, which not only maintains the same direction as $\mathbf{u}_c$, but also attempts to preserve the direction of the resultant rate of change of the state so that the direction of the resultant rate of change of the state is the same as that of the desired rate.

Consider Fig. 3 in which the plant is of the form $\dot{\mathbf{x}} = A\mathbf{x}+B\mathbf{u}$ and the desired control required to track the reference trajectory, $\mathbf{u}_{\text{desired}}$, is calculated. If $\mathbf{u}_{\text{desired}}$ is outside the control bounds, the saturated version of the control $\mathbf{u}_{\text{sat}}$ is applied. In Fig. 3(a), each component of $\mathbf{u}_{\text{desired}}$ is saturated to its respective maximum value. Consequently, $\mathbf{u}_{\text{sat}}$ has a different direction compared to $\mathbf{u}_{\text{desired}}$, and the resultant direction of $\dot{\mathbf{x}}_{\text{sat}}$ is different from $\dot{\mathbf{x}}_{\text{desired}}$. In Fig. 3(b), the saturation is enforced in such a way that the direction of $\mathbf{u}_{\text{sat}}$ is the same as that of $\mathbf{u}_{\text{desired}}$.

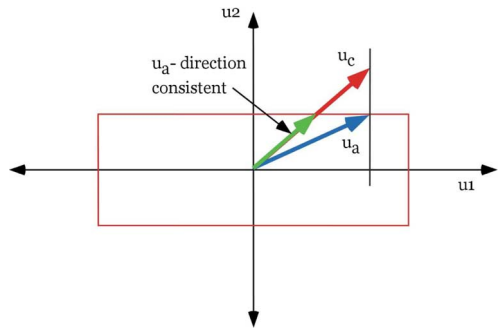

Fig. 2. Direction consistent control constraint mechanism.

However, the preservation of the control direction does not ensure that the resultant direction of $\dot{\mathbf{x}}_{\text{sat}}$ is the same as that of $\dot{\mathbf{x}}_{\text{desired}}$.

The control is calculated in two parts. The control necessary to cancel the inherent plant dynamics is calculated first, and then the control which produces a rate of change of the state in the desired direction is calculated. Referring to Fig. 3(c), the first component of the calculated control is equal to $-A\mathbf{x}$, and the second part is equal to $\dot{\mathbf{x}}_{\text{desired}}$. The first part of the calculated control will be within the control position limits since the plant state is restricted within the DCA. The second part of the control is subjected to direction consistent control saturation, which preserves the direction of the control vector. Therefore, the saturated version of the second part of the control equals $\dot{\mathbf{x}}_{\text{sat}}$, which also ensures that the direction of the resultant rate of change of the state is the same as the desired rate.

V. Tracking Control Law

The plant model is of the form given by (1)

$$\dot{\mathbf{x}} = \bar{A}\mathbf{x} + \bar{B}\mathbf{u}_a \tag{13}$$

where $\bar{A}$ and $\bar{B}$ are known constant matrices of compatible dimensions and the following assumptions hold.

Assumption A1: $\bar{B}$ is non-singular.

Assumption A2: The initial condition $\mathbf{x}_0 \in \mathbb{R}^n$ is such that $\nu \doteq \bar{B}^{-1}\bar{A}\mathbf{x}_0$ satisfies $|\nu_k| < u_{m_k}$ for all $k = 1, 2, \ldots, n$.

From this condition, due to continuity, there always exists a scalar $\lambda > 0$ such that $\nu_s = \bar{B}^{-1}(\bar{A} + \lambda I)\mathbf{x}_0$ also satisfies $|\nu_{s_k}| < u_{m_k}$ for all $k = 1, 2, \ldots, n$.

Assumption A3: We assume here that $\lambda > 0$ is chosen such that $|\nu_{s_k}| < u_{m_k}$ holds.

The tracking error is defined as

$$\mathbf{e}(t) = \mathbf{x}(t) - \mathbf{x}_r(t). \tag{14}$$

Differentiating the tracking error with respect to time, and substituting (13) into (14),

$$\dot{\mathbf{e}} = \bar{A}\mathbf{x} + \bar{B}\mathbf{u}_a - \dot{\mathbf{x}}_r. \tag{15}$$

Adding and subtracting $\lambda\mathbf{e}$ to (15), the equation for the error dynamics becomes

$$\dot{\mathbf{e}} = -\lambda\mathbf{e} + (\bar{A} + \lambda I)\mathbf{x} + \bar{B}\mathbf{u}_a - (\dot{\mathbf{x}}_r + \lambda\mathbf{x}_\mathbf{r}). \tag{16}$$

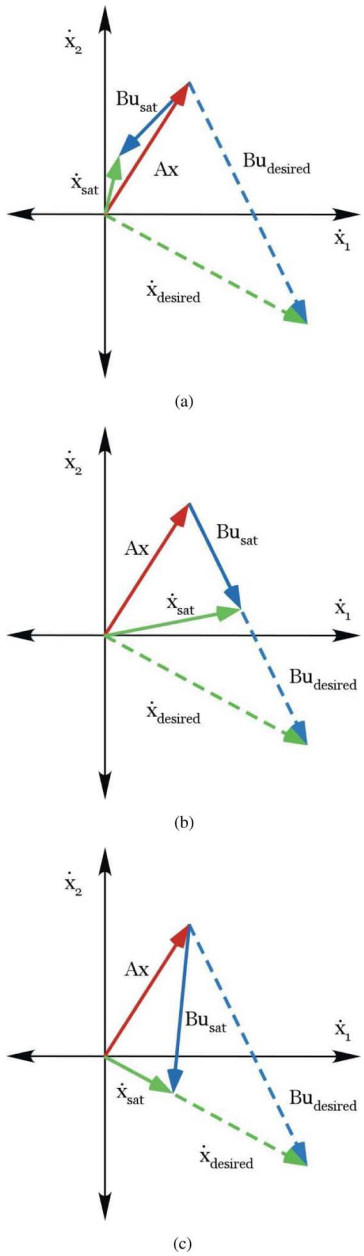

Fig. 3. Rate of change of the state due to various control saturation strategies. (a) Each component saturated to maximum. (b) Direction consistent control preserving the direction of the control vector. (c) Direction consistent control preserving the direction of the resultant rate of change of the state.

If

$$\mathbf{u}_a = -\bar{B}^{-1}(\bar{A} + \lambda I)\mathbf{x} + \bar{B}^{-1}(\dot{\mathbf{x}}_r + \lambda \mathbf{x_r}) \tag{17}$$

we have $\dot{\mathbf{e}} = -\lambda \mathbf{e}$. The parameter λ thus governs the closed-loop dynamic system behaviour and needs to be chosen appropriately such that assumptions A2 and A3 are satisfied. We now state the following definitions:

$$\mathbf{u}_t = -\bar{B}^{-1}(\bar{A} + \lambda I)\mathbf{x} + \bar{B}^{-1}(\dot{\mathbf{x}}_r + \lambda \mathbf{x_r}) \tag{18}$$

and

$$\mathbf{u}_s = -\bar{B}^{-1}(\bar{A} + \lambda I)\mathbf{x}. \tag{19}$$

Note that (18), referred in this work as the tracking control, has two components. The first term $-\bar{B}^{-1}(\bar{A} + \lambda I)\mathbf{x}$ cancels the inherent plant dynamics. The second term $\bar{B}^{-1}(\dot{\mathbf{x}}_r + \lambda \mathbf{x}_r)$ prescribes the desired dynamics necessary to track the reference trajectory. The first component is used as a measure of how close the state is to the DCA boundary and will be referred to as the stability control $\mathbf{u}_s$ defined by (19).

Further, define for each kth control input

$$u_{p_k} = \frac{|u_{s_k}|}{u_{m_k}} \tag{20}$$

where $k = 1, 2, 3, \ldots, n$. Then, the maximum of this ratio of stability control to the bound on each kth actuator is defined as

$$\mathbf{u}_{m_p} = \max(u_{p_1}, u_{p_2}, \ldots, u_{p_n}). \tag{21}$$

The quantity $\mathbf{u}_{m_p}$ is used as a measure of how close the current state is to the DCA boundary. Given the definition of $\mathbf{u}_{m_p}$ by virtue of (A3), we are ensured of $\mathbf{u}_{m_p}(0) < 1$. It should be noted that a value of $\mathbf{u}_{m_p} = 1$ indicates that the state is at the DCA boundary.

For a point which is inside the DCA, but approaching the boundary, the magnitude of $\mathbf{u}_{m_p}$ keeps increasing from 0 and reaches 1 on the boundary. To avoid saturation, choose scalar parameters s_1, s_2, p_1, and p_2 all close to 1, satisfying $0 < \mathbf{u}_{m_p}(0) < s_1 < s_2 < p_1 < p_2 < 1$ that decide the switch between tracking and stability control. Whenever, $\mathbf{u}_{m_p} > s_2$, the tracking control is close to being subjected to saturation. In this case, the concept of direction consistent control mechanism is implemented and the saturated version of the tracking control law is employed, given by the following equation:

$$\mathbf{u}_{t_{\text{sat}}} = -\bar{B}^{-1}(\bar{A}+\lambda I)\mathbf{x} + (1-\mathbf{u}_{m_p})\text{Sat}_{dc}\left\{\bar{B}^{-1}(\dot{\mathbf{x}}_r + \lambda \mathbf{x_r})\right\}. \tag{22}$$

The direction consistent control saturation function Sat_{dc} maintains the direction of the resultant control to be the same as the direction of the desired control in spite of control saturation. The saturation function is defined in Section V-A.

A. Saturation Function Definitions

For any $\mathbf{u}_{\text{des}} \in \mathbb{R}^n$, we adopt a hard saturation

$$\mathcal{S}(\mathbf{u}_{\text{des}_k}) = \min(\mathbf{u}_{m_k}, |\mathbf{u}_{\text{des}_k}|)\text{sgn}(\mathbf{u}_{\text{des}_k}) \tag{23}$$

for all $k = 1, 2, \ldots, n$ or alternately, a "soft" saturation of the form

$$\mathcal{S}(\mathbf{u}_{\text{des}_k}) = \tanh\left(\frac{\beta \mathbf{u}_{\text{des}_k}}{\mathbf{u}_{m_k}}\right)\mathbf{u}_{m_k} \tag{24}$$

for all $k = 1, 2, \ldots, n$, where β is any positive scalar parameter. Qualitatively, $\beta \to \infty$ implies that the "soft" saturation approaches the "hard" saturation definition stated earlier. If each of the controls is allowed to saturate independently to the maximum allowed value, the applied control is

$$\mathbf{u}_{\text{app}_k} = \mathcal{S}(\mathbf{u}_{\text{des}_k}), \quad \text{for all} \quad k = 1, 2, \ldots, n \tag{25}$$

where $\mathcal{S}$ is the saturation function. If direction consistency is to be maintained, the proportion p_k to which each control is saturated is calculated by

$$q_k = \frac{\mathcal{S}(u_{\text{des}_k})}{u_{\text{des}_k}}, \quad \text{for all} \quad k = 1, 2, \ldots, n. \tag{26}$$

The minimum saturation proportion $q_{\min}$ is identified

$$q_{\min} = \min(q_1, q_2, \ldots, q_n) \tag{27}$$

and all controls are saturated with the same proportion. Note, by construction $q_k < 1$ for all k and accordingly, $q_{\min} < 1$ also holds. As a result, the direction of the applied control vector is the same as the calculated control vector $\mathbf{u}_{\rm des}$. Therefore

$$\mathrm{Sat}_{dc}(\mathbf{u}_{\rm des}) = q_{\min}\mathbf{u}_{\rm des}. \tag{28}$$

B. Complete Control Law

Continuing with the discussion of $\mathbf{u}_{m_p}$, whenever its value is greater than p_2 the stability control is employed. The other design parameters s_1 and p_1 are used in order to produce smooth transitions between controls; from $\mathbf{u_t}$ and $\mathbf{u}_{\mathbf{t}_{\rm sat}}$, and from $\mathbf{u}_{\mathbf{t}_{\rm sat}}$ to $\mathbf{u_s}$. This transition can be accomplished by a linear or higher-order interpolation as $\mathbf{u}_{m_p}$ takes values from s_1 to s_2 and p_1 to p_2. Finally, the applied control $\mathbf{u}_a$ is defined as

$$\begin{aligned}\mathbf{u}_a &= \mathbf{u}_t \text{ if } |\mathbf{u}_{t_k}| < \mathbf{u}_{m_k} \text{ and } \mathbf{u}_{m_p} < s_1 \forall\ k = 1, 2, \ldots, n\\ &\quad \text{else,}\\ \mathbf{u}_a &= \begin{cases} \mathbf{u}_b, & \text{if } s_1 \le \mathbf{u}_{m_p} < s_2\\ \mathbf{u}_{t_{\rm sat}}, & \text{if } s_2 \le \mathbf{u}_{m_p} < p_1\\ \mathbf{u}_c, & \text{if } p_1 \le \mathbf{u}_{m_p} < p_2\\ \mathbf{u}_s, & \text{if } \mathbf{u}_{m_p} \ge p_2 \end{cases}\end{aligned} \tag{29}$$

where

$$\mathbf{u}_b = f(\mathbf{u}_t, \mathbf{u}_{t_{\rm sat}}, s_1, s_2, \mathbf{u}_{m_p}) \tag{30}$$

$$\mathbf{u}_c = f(\mathbf{u}_{t_{\rm sat}}, \mathbf{u}_s, p_1, p_2, \mathbf{u}_{m_p}) \tag{31}$$

have been introduced for smooth transitions between controls. The function f is a third-order interpolation scheme defined as

$$\begin{aligned} f(\mathbf{u}_1, \mathbf{u}_2, c_1, c_2, \mathbf{u}_{m_p}) &= \mathbf{u}_1 + (3\xi^2 - 2\xi^3)(\mathbf{u}_2 - \mathbf{u}_1)\\ \xi &= \frac{\mathbf{u}_{m_p} - c_1}{c_2 - c_1}. \end{aligned} \tag{32}$$

Next, it is shown that selecting p_2 such that $\mathbf{u}_{m_p}(0) < p_2 < 1$ ensures that $\mathbf{u}_{m_p}(t) \le p_2 \forall\ t$. This can be proved as follows. Let $\mathbf{u}_{m_p} < p_2$ for some $t = t_1 > 0$ and let $\mathbf{u}_{t_k} < \mathbf{u}_{m_k}$ and $\mathbf{u}_{m_p} < s_1$, then the applied control $\mathbf{u}_a = \mathbf{u}_t$. Then for $t > t_1$, $x(t) = e^{-\lambda(t-t_1)}x(t_1) + \text{function}(x_r, \dot{x}_r, \lambda)$ and $\mathbf{u}_{m_p}(t) = e(-\lambda(t-t_1))\mathbf{u}_{m_p}(t_1) + \text{function}(x_r, \dot{x}_r, \lambda, \bar{A}, \bar{B})$. If $\mathbf{u}_{m_p}(t) > s_1$ the control smoothly switches to $\mathbf{u}_b$. The control continues to switch from there on depending on the value of parameter $\mathbf{u}_{m_p}$. Suppose there exists a finite time $t^* > 0$ such that $\mathbf{u}_{m_p}(t^*) = p_2$ and $\mathbf{u}_{m_p}(t) \ge p_2, \forall\ t > t^*$. Then, $\mathbf{u}_a(t) = \mathbf{u}_s(t) = -\bar{B}^{-1}(\bar{A} + \lambda I)\mathbf{x}(t) \quad \forall\ t \ge t^*$. This would yield

$$\mathbf{x}(t) = \mathbf{x}(t^*)e^{-\lambda(t-t^*)} \quad \forall\ t \ge t^*. \tag{33}$$

Using the definition of $\mathbf{u}_{m_p}(t)$ we have for all time

$$\mathbf{u}_{m_p}(t) = e^{-\lambda(t-t^*)}\mathbf{u}_{m_p}(t^*) \tag{34}$$

$$= e^{-\lambda(t-t^*)}p_2 \quad \le p_2 \tag{35}$$

which is a contradiction. Thus, $\mathbf{u}_{m_p}(t) \le p_2$ for all time $t \ge 0$. Finally, note that the closed-loop tracking error system is given by

$$\dot{\mathbf{e}} = -\lambda\mathbf{e} + \bar{B}\delta \tag{36}$$

where δ is a bounded signal of time whose explicit characterization is

$$\delta = \begin{cases} 0, & \text{if } |\mathbf{u}_{t_k}| < \mathbf{u}_{m_k} \text{ and } \mathbf{u}_{m_p} < s_1\\ \mathbf{u}_b - \mathbf{u}_t, & \text{if } s_1 \le \mathbf{u}_{m_p} < s_2\\ \mathbf{u}_{t_{\rm sat}} - \mathbf{u}_t, & \text{if } s_2 \le \mathbf{u}_{m_p} < p_1\\ \mathbf{u}_c - \mathbf{u}_t, & \text{if } p_1 \le \mathbf{u}_{m_p} < p_2\\ \mathbf{u}_s - \mathbf{u}_t, & \text{if } \mathbf{u}_{m_p} \ge p_2 \end{cases} \tag{37}$$

or

$$\begin{aligned}\delta &= 0, \quad \text{if} |\mathbf{u}_{t_k}| < \mathbf{u}_{m_k} \text{and} \mathbf{u}_{m_p} < s_1 \qquad (38)\\ \delta &= (3\xi^2 - 2\xi^3)((1 - \mathbf{u}_{m_p})\mathrm{Sat}_{dc}(\bar{B}^{-1}(\dot{\mathbf{x}}_r + \lambda\mathbf{x_r})))\\ &\quad - (3\xi^2 - 2\xi^3)\bar{B}^{-1}(\dot{\mathbf{x}}_r + \lambda\mathbf{x_r}),\\ &\text{if } s_1 \le \mathbf{u}_{m_p} < s_2, \text{ where } \xi = \frac{\mathbf{u}_{m_p} - s_1}{s_2 - s_1} \qquad (39)\\ \delta &= (1 - \mathbf{u}_{m_p})\mathrm{Sat}_{dc}(\bar{B}^{-1}(\dot{\mathbf{x}}_r + \lambda\mathbf{x_r}))\\ &\quad - (\bar{B}^{-1}(\dot{\mathbf{x}}_r + \lambda\mathbf{x}_r)),\\ &\text{if } s_2 \le \mathbf{u}_{m_p} < p_1 \qquad (40)\\ \delta &= (1 - \mathbf{u}_{m_p})\mathrm{Sat}_{dc}(\bar{B}^{-1}(\dot{\mathbf{x}}_r + \lambda\mathbf{x_r}))\\ &\quad - (\bar{B}^{-1}(\dot{\mathbf{x}}_r + \lambda\mathbf{x_r}))\\ &\quad + (3\xi^2 - 2\xi^3)\left((1 - \mathbf{u}_{m_p})\mathrm{Sat}_{dc}(\bar{B}^{-1}(\dot{\mathbf{x}}_r + \lambda\mathbf{x_r}))\right),\\ &\text{if } p_1 \le \mathbf{u}_{m_p} < p_2, \text{ where } \xi = \frac{\mathbf{u}_{m_p} - p_1}{p_2 - p_1} \qquad (41)\\ \delta &= -(\bar{B}^{-1}(\dot{\mathbf{x}}_r + \lambda\mathbf{x}_r)) \text{ if } \mathbf{u}_{m_p} \ge p_2. \qquad (42)\end{aligned}$$

Due to boundedness for δ, we have $\mathbf{e} \in \mathcal{L}_\infty$ ensuring boundedness for all closed-loop signals.

VI. Adaptive Case

Before proceeding to the control law for the case of uncertain parameters, the following assumption is made.

Assumption B1: Both B and $\bar{B}$ are non-singular. Further, suppose there exists a symmetric matrix L that is either positive or negative definite such that $LB = \bar{B}$, or

$$L = [I + \Delta B\bar{B}^{-1}]^{-1}. \tag{43}$$

Assume also that the function $\mathrm{sgn}(L)$ is known and defined such that $\mathrm{sgn}(L) = 1$ when L is positive definite, and $\mathrm{sgn}(L) = -1$ when L is negative definite. Additionally define matrix P,

$$P = L\mathrm{sgn}(L) \tag{44}$$

and let $p_M = \underset{\triangle B}{\lambda_{\max}}[P]$ and $p_m = \underset{\triangle B}{\lambda_{\min}}[P]$ be the maximum and minimum eigenvalues of P, respectively.

Define $\theta = B^{-1}(A + \lambda I)$, $\bar{\theta} = \bar{B}^{-1}(\bar{A} + \lambda I)$, $\phi = B^{-1}$, and $\bar{\phi} = \bar{B}^{-1}$, where λ is the specified closed-loop eigenvalue as

defined in earlier section. Thus $\phi = (\bar{B} + \triangle B)^{-1}$, and through the application of the matrix-inversion lemma

$$\phi = \bar{B}^{-1} - (\bar{B} + \triangle B)^{-1} \triangle B \bar{B}^{-1} \tag{45}$$
$$= \bar{\phi} + \triangle\phi \tag{46}$$

where $\triangle\phi = -(\bar{B} + \triangle B)^{-1} \triangle B \bar{B}^{-1}$. Now, given $\bar{B}$ and the fact that the uncertainty $\triangle B$ satisfies $B_{ij} = \bar{B}_{ij} + \triangle B_{ij}$ from (3), we denote

$$\triangle\phi_{ij}{}^{\max} = \max_{\triangle B} [\triangle\phi_{ij}]$$
$$\triangle\phi_{ij}{}^{\min} = \min_{\triangle B} [\triangle\phi_{ij}]. \tag{47}$$

Thus, we have

$$\phi_{ij} \in \left[\bar{\phi}_{ij} - \triangle\phi_{ij}{}^{\min}, \bar{\phi}_{ij} + \triangle\phi_{ij}{}^{\max}\right] \tag{48}$$

wherein the values of $\triangle\phi_{ij}{}^{\min}$ and $\triangle\phi_{ij}{}^{\max}$ can be precomputed as well-posed optimization problems represented via (47). Then the feasible set of values for ϕ may be defined as

$$\phi_f = \phi \in \mathbb{R}^{n\times n}$$
$$\text{such that } \phi_{ij} \in \left[\bar{\phi}_{ij} + \triangle\phi_{ij}{}^{\min}, \bar{\phi}_{ij} + \triangle\phi_{ij}{}^{\max}\right]. \tag{49}$$

Similarly, for $\theta = B^{-1}(A + \lambda I)$, we can obtain

$$\theta = [\bar{B}^{-1}(\bar{A} + \lambda I + \triangle A)] - (\bar{B} + \triangle B)^{-1} \triangle B \bar{B}^{-1} (\bar{A} + \lambda I + \triangle A)$$
$$= \bar{B}^{-1}(\bar{A} + \lambda I) + \bar{B}^{-1}\triangle A - (\bar{B} + \triangle B)^{-1} \triangle B \bar{B}^{-1} [\bar{A} + \lambda I + \triangle A]$$
$$= \bar{\theta} + \triangle\theta \tag{50}$$

where $\triangle\theta = \bar{B}^{-1}\triangle A - (\bar{B} + \triangle B)^{-1} \triangle B \bar{B}^{-1} [\bar{A} + \lambda I + \triangle A]$. For any given $\bar{A}$, $\bar{B}$, and $\lambda > 0$ and for uncertainties $\triangle A$ and $\triangle B$ subject to (2) and (3) we can again predetermine

$$\triangle\theta_{ij}{}^{\max} = \max_{\triangle A, \triangle B} [\triangle\theta_{ij}]$$
$$\triangle\theta_{ij}{}^{\min} = \min_{\triangle A, \triangle B} [\triangle\theta_{ij}] \tag{51}$$

such that

$$\theta_{ij} \in \left[\bar{\theta}_{ij} + \triangle\theta_{ij}{}^{\min}, \bar{\theta}_{ij} + \triangle\theta_{ij}{}^{\max}\right]. \tag{52}$$

As before, the feasible set of values for θ can be defined as

$$\theta_f = \left\{\theta \in \mathbb{R}^{n\times n} | \theta_{ij} \in \left[\bar{\theta}_{ij} - \triangle\theta_{ij}{}^{\min}, \bar{\theta}_{ij} + \triangle\theta_{ij}{}^{\max}\right]\right\}. \tag{53}$$

Further, define column vector complements of the matrices ϕ and θ

$$\phi_v = [\phi_{11}, \ldots, \phi_{1n}, \phi_{21}, \ldots, \phi_{2n}, \phi_{n1}, \ldots, \phi_{nn}]^T \tag{54}$$
$$\theta_v = [\theta_{11}, \ldots, \theta_{1n}, \theta_{21}, \ldots, \theta_{2n}, \theta_{n1}, \ldots, \theta_{nn}]^T \tag{55}$$

with each row of θ defined as

$$\chi_k = [\theta_{k1}, \theta_{k2}, \ldots, \theta_{kn}] \text{ for all } k = 1, \ldots, n. \tag{56}$$

Assumption B2: We denote $\tilde{\nu}_s = -\hat{\theta}(0)\mathbf{x}_0$, where the *hat* over the variable denotes its estimated value. From (56), $\tilde{\nu}_{s,k} = -\hat{\chi}_k(0)\mathbf{x}_0$ and for any given $\mathbf{x}_0 \in \mathbb{R}^n$

$$|\tilde{\nu}_{s,k}| = |\hat{\chi}_k(0)\mathbf{x}_0| \tag{57}$$
$$\leq \max_{\theta_f} \|\chi_k\|_1 \|\mathbf{x}_0\|_\infty \tag{58}$$
$$\leq \mu_k \|\mathbf{x}_0\| \tag{59}$$

with $\mu_k = \max_{\theta_f} \|\hat{\chi}_k\|_1$. Assume that for any $\mathbf{x}_0 \in \mathbb{R}^n$, $\mu_k \|\mathbf{x}_0\| \leq \alpha p_2 \mathbf{u}_{m_k}$ for all $k = 1, 2, \ldots, n$. For some p_2 selected such that $0 \ll p_2 < 1$, select the scalar α such that

$$\alpha = \min_k \sqrt{\frac{p_m}{p_M \beta_k} - \frac{\Theta \mu_k}{\gamma p_2^2 p_M \beta_k \mathbf{u}_{m_k}^2}} \tag{60}$$

$$\text{with } \Theta = \sum_{i=1}^{n}\sum_{j=1}^{n} \left(\Delta\theta_{ij}^{\max} + \Delta\theta_{ij}^{\min}\right)^2 \tag{61}$$

$$\text{and } \beta_k = \frac{\max_{\theta_f} \|\chi_k\|_1^2}{\min_{\theta_f} \|\chi_k\|_1^2} \tag{62}$$

for all $k = 1, 2, \ldots, n$. Note that this assumption is more conservative than non-adaptive case.

Following the control law formulation laid out in the previous section, but this time written in terms of θ and ϕ

$$\dot{\mathbf{e}} = -\lambda\mathbf{e} + B(\mathbf{u}_a + \theta\mathbf{x} - \phi(\dot{\mathbf{x}}_r + \lambda\mathbf{x}_\mathbf{r})). \tag{63}$$

For systems with unknown θ and ϕ matrices, the control law is defined as

$$\mathbf{u}_a = \mathbf{u}_t \text{ if } |\mathbf{u}_{t_k}| < \mathbf{u}_{m_k} \text{ and } \mathbf{u}_{m_p} < s_1 \forall\, k = 1, \ldots n$$
$$\text{else,}$$
$$\mathbf{u}_a = \begin{cases} \mathbf{u}_b, & \text{if } s_1 \leq \mathbf{u}_{m_p} < s_2 \\ \mathbf{u}_{t_{\text{sat}}}, & \text{if } s_2 \leq \mathbf{u}_{m_p} < p_1 \\ \mathbf{u}_c, & \text{if } p_1 \leq \mathbf{u}_{m_p} < p_2 \\ \mathbf{u}_s, & \text{if } \mathbf{u}_{m_p} \geq p_2 \end{cases} \tag{64}$$

where

$$\mathbf{u}_t = -\hat{\theta}\mathbf{x} + \hat{\phi}(\dot{\mathbf{x}}_r + \lambda\mathbf{x}_\mathbf{r}) \tag{65}$$
$$\mathbf{u}_s = -\hat{\theta}\mathbf{x} \tag{66}$$
$$\mathbf{u}_{t_{\text{sat}}} = -\hat{\theta}\mathbf{x} + (1 - \mathbf{u}_{m_p})\mathbf{Sat}_\mathbf{dc}(\hat{\phi}(\dot{\mathbf{x}}_r + \lambda\mathbf{x}_\mathbf{r})) \tag{67}$$

$\mathbf{u}_b$ and $\mathbf{u}_c$ are given in (30) and (31) and $\hat{\theta}$ and $\hat{\phi}$ are estimated values of θ and ϕ. It is important to point that in this case the definition of $\mathbf{u}_{m_p}$ is revised to

$$\mathbf{u}_{m_p} = \max_k [\mathbf{u}_{p,k}] \tag{68}$$
$$\mathbf{u}_{p_k} = \frac{\|\hat{\chi}_k\|_1 \|\mathbf{x}\|}{\alpha \mathbf{u}_{m_k}} \tag{69}$$

where $k = 1, 2, 3, \ldots, n$. Substituting for the control law defined in (64), the closed-loop error dynamics reduce to

$$\dot{\mathbf{e}} = -\boldsymbol{\lambda}\mathbf{e} - B(\hat{\theta} - \theta)\mathbf{x} + B(\hat{\phi} - \phi)(\dot{\mathbf{x}}_r + \lambda\mathbf{x}_\mathbf{r}) + B\delta \tag{70}$$

where

$$\delta = \mathbf{u}_a - \mathbf{u}_t \tag{71}$$

that is

$$\delta = 0 \text{ if } |\mathbf{u}_{t_k}| < \mathbf{u}_{m_k} \text{and} \mathbf{u}_{m_p} < s_1 \tag{72}$$

$$\begin{aligned}\delta =& (3\xi^2 - 2\xi^3)((1 - \mathbf{u}_{m_p})\mathrm{Sat}_{dc}(\hat{\phi}(\dot{\mathbf{x}}_r + \lambda \mathbf{x_r}))) \\ &- (3\xi^2 - 2\xi^3)\hat{\phi}(\dot{\mathbf{x}}_r + \lambda \mathbf{x_r})\end{aligned}$$

$$\text{if } s_1 \leq \mathbf{u}_{m_p} < s_2, \text{ where } \xi = \frac{\mathbf{u}_{m_p} - s_1}{s_2 - s_1} \tag{73}$$

$$\delta = (1 - \mathbf{u}_{m_p})\mathrm{Sat}_{dc}(\hat{\phi}(\dot{\mathbf{x}}_r + \lambda \mathbf{x_r})) - (\hat{\phi}(\dot{\mathbf{x}}_r + \lambda \mathbf{x_r}))$$

$$\text{if } s_2 \leq \mathbf{u}_{m_p} < p_1 \tag{74}$$

$$\begin{aligned}\delta =& (1 - \mathbf{u}_{m_p})\mathrm{Sat}_{dc}(\hat{\phi}(\dot{\mathbf{x}}_r + \lambda \mathbf{x_r})) - (\hat{\phi}(\dot{\mathbf{x}}_r + \lambda \mathbf{x_r})) \\ &+ (3\xi^2 - 2\xi^3)\left((1 - \mathbf{u}_{m_p})\mathrm{Sat}_{dc}(\hat{\phi}(\dot{\mathbf{x}}_r + \lambda \mathbf{x_r}))\right)\end{aligned}$$

$$\text{if } p_1 \leq \mathbf{u}_{m_p} < p_2, \text{ where } \xi = \frac{\mathbf{u}_{m_p} - p_1}{p_2 - p_1} \tag{75}$$

$$\delta = -(\hat{\phi}(\dot{\mathbf{x}}_r + \lambda \mathbf{x_r})) \text{ if } \mathbf{u}_{m_p} \geq p_2 \tag{76}$$

or

$$\delta = \delta(\hat{\phi}, \mathbf{x}_r, \dot{\mathbf{x}}_r) \text{ for all } \mathbf{u}_{m_p}. \tag{77}$$

In terms of column vector complements defined in (56)–(57), rewrite the closed-loop error dynamics as

$$\dot{\mathbf{e}} = -\boldsymbol{\lambda}\mathbf{e} - B\Lambda_x(\hat{\theta}_v - \theta_v) + B\Omega(\hat{\phi}_v - \phi_v) + B\delta \tag{78}$$

with terms Λ_x and Ω defined such that

$$\Lambda_x(\hat{\theta}_v - \theta_v) = (\hat{\theta} - \theta)\mathbf{x} \tag{79}$$

$$\Omega(\hat{\phi}_v - \phi_v) = (\hat{\phi} - \phi)(\dot{\mathbf{x}}_r + \lambda \mathbf{x_r}). \tag{80}$$

A. Adaptive Laws

To satisfy the given bounds on parameters and avoid parameter drift, the projection scheme from [21] is adopted

$$\hat{\theta}_{v,k} = \Gamma(\theta_{v,k}) \tag{81}$$

$$\hat{\phi}_{v,k} = \Gamma(\phi_{v,k}) \tag{82}$$

where Γ is defined as

$$\Gamma(\bullet) = \begin{cases} \breve{\bullet}, & \text{if } \breve{\bullet} \in (\bullet^{\min}, \bullet^{\max}) \\ \bullet^{\min}, & \text{if } \breve{\bullet} \leq \bullet^{\min} \\ \bullet^{\max}, & \text{if } \breve{\bullet} \geq \bullet^{\max}. \end{cases} \tag{83}$$

The adaptive laws selected to be

$$\begin{aligned}\dot{\breve{\theta}}_v =& \gamma {\Lambda_x}^T \bar{B}^T \mathbf{e}\, \mathrm{sgn}(L) - \gamma\sigma_1(\breve{\theta}_v - \hat{\theta}_v) \text{ if } \mathbf{u}_a \neq \mathbf{u}_s \\ \text{else } \dot{\breve{\theta}}_v =& \gamma {\Lambda_x}^T \bar{B}^T \mathbf{x}\, \mathrm{sgn}(L) - \gamma\sigma_1(\breve{\theta}_v - \hat{\theta}_v)\end{aligned} \tag{84}$$

and if at some $t = t_* \geq 0$, $\mathbf{u}_{m_p}(t_*) = p_2$, $\breve{\theta}(t_*) \neq \hat{\theta}(t_*^-)$, reset $\breve{\theta}(t)$ such that $\breve{\theta}(t_*) = \hat{\theta}(t_*^-)$.

$$\dot{\breve{\phi}}_v = -\gamma\Omega^T \bar{B}^T \mathbf{e}\, \mathrm{sgn}(L) - \gamma\sigma_2(\breve{\phi}_v - \hat{\phi}_v) \tag{85}$$

for any $\sigma_1, \sigma_2 > \lambda/\gamma$ and the adaptive gain γ is chosen to satisfy

$$\gamma > \max_k \left[\frac{\Theta\mu_k}{p_m p_2^2 \mathbf{u}_{m_k}^2}\right]. \tag{86}$$

B. Stability Analysis

To prove stability of the control laws in (64) and the adaptive laws specified in (84)–(85), choose the following Lyapunov function candidate:

$$\begin{aligned}V =& \mathbf{e}^T P \mathbf{e} + \frac{1}{\gamma}\left[\|\breve{\theta}_v - \theta_v\|^2 - \|\breve{\theta}_v - \hat{\theta}_v\|^2\right] \\ &+ \frac{1}{\gamma}\left[\|\breve{\phi}_v - \phi_v\|^2 - \|\breve{\phi}_v - \hat{\phi}_v\|^2\right].\end{aligned} \tag{87}$$

Details of the proof that this Lyapunov function is non-negative are presented in [21]. Now take the time derivative of (87), and noting that the true parameters are constant

$$\begin{aligned}\dot{V} =& -2\lambda \mathbf{e}^T P \mathbf{e} - 2\mathbf{e}^T P B \Lambda_x(\hat{\theta}_v - \theta_v) \\ &+ 2\mathbf{e}^T P \Omega(\hat{\phi}_v - \phi_v) + 2\mathbf{e}^T P B \delta \\ &+ \frac{2}{\gamma}\left[\dot{\breve{\theta}}_v^T(\breve{\theta}_v - \theta_v) - (\dot{\breve{\theta}}_v - \dot{\hat{\theta}}_v)^T(\breve{\theta}_v - \hat{\theta}_v)\right] \\ &+ \frac{2}{\gamma}\left[\dot{\breve{\phi}}_v^T(\breve{\phi}_v - \phi_v) - (\dot{\breve{\phi}}_v - \dot{\hat{\phi}}_v)^T(\breve{\phi}_v - \hat{\phi}_v)\right].\end{aligned} \tag{88}$$

For the case $\mathbf{u}_a \neq \mathbf{u}_s$ substitute for P from (44) and the adaptive laws from (84)–(85)

$$\begin{aligned}\dot{V} =& -2\lambda \mathbf{e}^T P \mathbf{e} + 2\mathbf{e}^T \bar{B} \delta\, \mathrm{sgn}(L) - 2\sigma_1(\breve{\theta}_v - \hat{\theta}_v)^T(\hat{\theta}_v - \theta_v) \\ &- 2\sigma_2(\breve{\phi}_v - \hat{\phi}_v)^T(\hat{\phi}_v - \phi_v).\end{aligned} \tag{89}$$

Using completion of squares

$$\begin{aligned}\dot{V} \leq& -\lambda \mathbf{e}^T P \mathbf{e} + \frac{\|\bar{B}\|^2 {\delta_M}^2}{\lambda p_m} - 2\sigma_1(\breve{\theta}_v - \hat{\theta}_v)^T(\hat{\theta}_v - \theta_v) \\ &- 2\sigma_2(\breve{\phi}_v - \hat{\phi}_v)^T(\hat{\phi}_v - \phi_v)\end{aligned} \tag{90}$$

where $\delta_M = \sup_t \|\delta(t)\|$. Note from (77) $\delta(t)$ is a function of $\hat{\phi}$ that is bounded due to the projection scheme adopted, reference trajectory $\mathbf{x}_r$ and its derivative $\dot{\mathbf{x}}_r$ that are bounded by choice and the parameter λ that is a positive scalar quantity chosen by the designer. By virtue of these signals, it is guaranteed that $\delta(t)$ is bounded for all time and its supremum exists. Furthermore

$$\begin{aligned}\dot{V} \leq& -\lambda \mathbf{e}^T P \mathbf{e} - \frac{\lambda}{\gamma}\left\{\|\breve{\theta}_v - \theta_v\|^2 - \|\breve{\theta}_v - \hat{\theta}_v\|^2\right\} \\ &- \frac{\lambda}{\gamma}\left\{\|\breve{\phi}_v - \phi_v\|^2 - \|\breve{\phi}_v - \hat{\phi}_v\|^2\right\} \\ &+ \frac{\lambda}{\gamma}\left\{\|\breve{\theta}_v - \theta_v\|^2 - \|\breve{\theta}_v - \hat{\theta}_v\|^2\right\} \\ &+ \frac{\lambda}{\gamma}\left\{\|\breve{\phi}_v - \phi_v\|^2 - \|\breve{\phi}_v - \hat{\phi}_v\|^2\right\} \\ &+ \frac{\|\bar{B}\|^2 {\delta_M}^2}{\lambda p_m} - 2\sigma_1(\breve{\theta}_v - \hat{\theta}_v)^T(\hat{\theta}_v - \theta_v) \\ &- 2\sigma_2(\breve{\phi}_v - \hat{\phi}_v)^T(\hat{\phi}_v - \phi_v).\end{aligned} \tag{91}$$

Since $\sigma_1 > \lambda/\gamma$ and $\sigma_2 > \lambda/\gamma$, we have

$$\begin{aligned}\dot{V} \leq& -\lambda V + \frac{\|\bar{B}\|^2 {\delta_M}^2}{\lambda p_m} \\ &+ \frac{\lambda}{\gamma}\sum_{k=1}^{n^2}(2\breve{\theta}_{v,k} - \theta_{v,k} - \hat{\theta}_{v,k})(\hat{\theta}_{v,k} - \theta_{v,k})\end{aligned}$$

$$- \frac{2\lambda}{\gamma}\sum_{k=1}^{n^2}(\hat{\theta}_{v,k}-\theta_{v,k})(\breve{\theta}_{v,k}-\hat{\theta}_{v,k}) + \frac{\lambda}{\gamma}\sum_{k=1}^{n^2}(2\breve{\phi}_{v,k}-\phi_{v,k}-\hat{\phi}_{v,k})(\hat{\phi}_{v,k}-\phi_{v,k}) - \frac{2\lambda}{\gamma}\sum_{k=1}^{n^2}(\hat{\phi}_{v,k}-\phi_{v,k})(\breve{\phi}_{v,k}-\hat{\phi}_{v,k}) \quad (92)$$

or

$$\dot{V} \leq -\lambda V + \frac{\|\bar{B}\|^2 {\delta_M}^2}{\lambda p_m} + \frac{\lambda}{\gamma}\sum_{k=1}^{n^2}(\hat{\theta}_{v,k}-\theta_{v,k})(\breve{\theta}_{v,k}-\theta_{v,k}) - \frac{\lambda}{\gamma}\sum_{k=1}^{n^2}(\hat{\theta}_{v,k}-\theta_{v,k})(\breve{\theta}_{v,k}-\hat{\theta}_{v,k}) + \frac{\lambda}{\gamma}\sum_{k=1}^{n^2}(\hat{\phi}_{v,k}-\phi_{v,k})(\breve{\phi}_{v,k}-\phi_{v,k}) - \frac{\lambda}{\gamma}\sum_{k=1}^{n^2}(\hat{\phi}_{v,k}-\phi_{v,k})(\breve{\phi}_{v,k}-\hat{\phi}_{v,k}). \quad (93)$$

Thus

$$\dot{V} \leq -\lambda V + \frac{\|\bar{B}\|^2 {\delta_M}^2}{\lambda p_m} + \frac{\lambda}{\gamma}\sum_{k=1}^{n^2}\left[(\hat{\theta}_{v,k}-\theta_{v,k})^2 + (\hat{\phi}_{v,k}-\phi_{v,k})^2\right] \quad (94)$$

or

$$\dot{V} \leq -\lambda V + \frac{\|\bar{B}\|^2 {\delta_M}^2}{\lambda p_m} + \frac{\lambda}{\gamma}\left[\sum_{i=1}^{n}\sum_{j=1}^{n}\left\{(\theta_{i,j}^{\max}-\theta_{v,k}^{\min})^2 + (\phi_{i,j}^{\max}-\phi_{v,k}^{\min})^2\right\}\right]. \quad (95)$$

Finally, it can be concluded that

$$\dot{V} \leq -\lambda V + \epsilon \quad (96)$$

for some positive constant ϵ. This ensures that the Lyapunov function V is uniformly bounded for the case $\mathbf{u}_a \neq \mathbf{u}_s$.

For the case $\mathbf{u}_a = \mathbf{u}_s$, there is an additional term in (89)

$$\dot{V} = -2\lambda\mathbf{e}^T P\mathbf{e} + 2\mathbf{e}^T\bar{B}\delta\,\mathrm{sgn}(L) - 2\sigma_1(\breve{\theta}_v-\hat{\theta}_v)^T(\hat{\theta}_v-\theta_v) - 2\sigma_2(\breve{\phi}_v-\hat{\phi}_v)^T(\hat{\phi}_v-\phi_v) + 2\mathbf{x}_r^T\bar{B}\Lambda_x(\hat{\theta}_v-\theta_v). \quad (97)$$

Now

$$2\mathbf{x}_r^T\bar{B}\Lambda_x(\hat{\theta}_v-\theta_v) = 2\mathbf{x}_r^T\bar{B}(\hat{\theta}-\theta)\mathbf{x} = 2\mathbf{x}_r^T\bar{B}(\hat{\theta}-\theta)\mathbf{x}_r + 2\mathbf{e}^T(\hat{\theta}-\theta)^T\bar{B}^T\mathbf{x}_r. \quad (98)$$

Define $\rho = \max_{\theta_1,\theta_2\in\theta_f}\|\theta_1-\theta_2\|$ and $x_{rm} = \sup_t\|\mathbf{x}_r(t)\|$. Then

$$\dot{V} \leq -\lambda\mathbf{e}^T P\mathbf{e} - 2\sigma_1(\breve{\theta}_v-\hat{\theta}_v)^T(\hat{\theta}_v-\theta_v) - 2\sigma_2(\breve{\phi}_v-\hat{\phi}_v)^T(\hat{\phi}_v-\phi_v) - \lambda\mathbf{e}^T P\mathbf{e} + 2\rho\|\bar{B}\|x_{rm}^2 + 2\mathbf{e}^T\bar{B}\delta\,\mathrm{sgn}(L) + 2\rho\|\mathbf{e}\|x_{rm}\|\bar{B}\| \quad (99)$$

or

$$\dot{V} \leq -\lambda\mathbf{e}^T P\mathbf{e} - 2\sigma_1(\breve{\theta}_v-\hat{\theta}_v)^T(\hat{\theta}_v-\theta_v) - 2\sigma_2(\breve{\phi}_v-\hat{\phi}_v)^T(\hat{\phi}_v-\phi_v) - \lambda\mathbf{e}^T p_m\|\mathbf{e}\|^2 + 2\rho\|\bar{B}\|x_{rm}^2 + 2\|\mathbf{e}\|\|\bar{B}\|[\delta_M+\rho x_{rm}]. \quad (100)$$

Let $\tilde{\delta}_m = \delta_M + \rho x_{rm}$, and replicate steps (91)–(94), to get

$$\dot{V} \leq -\lambda V + \frac{\|\bar{B}\|^2\tilde{\delta}_m^2}{\lambda p_m} + 2\rho\|\bar{B}\|x_{rm}^2 + \frac{\lambda}{\gamma}\sum_{i=1}^{n}\sum_{j=1}^{n}\left[\left(\theta_{ij}^{\max}-\theta_{ij}^{\min}\right)^2 + \left(\phi_{ij}^{\max}-\phi_{ij}^{\min}\right)^2\right]. \quad (101)$$

Similar to (96), it can be concluded that

$$\dot{V} \leq -\lambda V + \tilde{\epsilon} \quad (102)$$

for some other finite positive constant $\tilde{\epsilon}$. Therefore, from the uniform boundedness theorem, one concludes that $\mathbf{e} \in \mathcal{L}_\infty$, $\breve{\theta} \in \mathcal{L}_\infty$ and $\breve{\phi} \in \mathcal{L}_\infty$, which results in the boundedness of all closed-loop signals.

C. Control Saturation Analysis

The next issue to be analyzed is whether the control signal stays within saturation limits for all time. Suppose that at some time $t = t_* \geq 0$, $\mathbf{u}_{m_p}(t_*) = p_2$ such that, $\mathbf{u}_a(t_*^+) = \mathbf{u}_s(t_*^+)$. In this case

$$\|\hat{\chi}_k(t_*)\|_1^2\|\mathbf{x}(t_*)\|^2 \leq \alpha^2 {p_2}^2 {\mathbf{u}_{m_k}}^2 \quad (103)$$

from the definition of $\mathbf{u}_{m_p}$ in (68).

For time $t \geq t_*$, suppose that $\mathbf{u}_a = \mathbf{u}_s$, then the state evolves according to

$$\dot{\mathbf{x}} = -\lambda\mathbf{x} - B\Lambda_x(\hat{\theta}_v-\theta_v). \quad (104)$$

Consider the Lyapunov function candidate

$$V_s = \mathbf{x}^T P\mathbf{x} + \frac{1}{\gamma}\left[\|\breve{\theta}_v-\theta_v\|^2 - \|\breve{\theta}_v-\hat{\theta}_v\|^2\right]. \quad (105)$$

Notice that the form of (105) is similar to (87), and it can be verified that V_s is positive definite. Next, take the derivative of V_s along the trajectory in (104) to get

$$\dot{V}_s = 2\mathbf{x}^T P\left[-\lambda\mathbf{x} - B\Lambda_x(\hat{\theta}_v-\theta_v)\right] + \frac{2}{\gamma}(\hat{\theta}_v-\theta_v)\dot{\breve{\theta}}_v^T. \quad (106)$$

Substituting the adaptive law for $\dot{\breve{\theta}}_v$ in (84)

$$\dot{V}_s = -2\lambda\mathbf{x}^T P\mathbf{x} - 2\mathbf{x}^T\bar{B}\Lambda_x(\hat{\theta}_v-\theta_v)\mathrm{sgn}(L) + \frac{2}{\gamma}(\hat{\theta}_v-\theta_v)\left[\gamma{\Lambda_x}^T\bar{B}^T\mathbf{x}\,\mathrm{sgn}(L) - \gamma\sigma_1(\breve{\theta}_v-\hat{\theta}_v)\right]^T \quad (107)$$

$$\dot{V}_s = -2\lambda\mathbf{x}^T P\mathbf{x} - 2\sigma_1(\breve{\theta}_v-\hat{\theta}_v)^T(\hat{\theta}_v-\theta_v) \leq 0. \quad (108)$$

Thus, one can conclude $V_s(t) \leq V_s(t_*)$ for $t \geq t_*$. Further

$$p_m \|\mathbf{x}(t)\|^2 \leq \mathbf{x}^T(t) P \mathbf{x}(t) \leq V_s(t) \leq V_s(t_*). \tag{109}$$

But

$$\begin{aligned} V_s(t_*) &= \mathbf{x}^T(t_*) P \mathbf{x}(t_*) + \frac{1}{\gamma} \|\hat{\theta}_v - \theta_v\|^2 \\ V_s(t_*) &\leq p_M \|\mathbf{x}(t_*)\|^2 + \frac{\Theta}{\gamma}. \end{aligned} \tag{110}$$

Combining (109) and (110)

$$\begin{aligned} \|\mathbf{x}(t)\|^2 &\leq \frac{p_M}{p_m} \|\mathbf{x}(t_*)\|^2 + \frac{\Theta}{\gamma p_m} \\ &\leq \frac{p_M}{p_m} \frac{1}{\min_{\theta_f} \|\chi_k\|_1^2} \|\chi_k(t_*)\|_1{}^2 \|\mathbf{x}(t_*)\|^2 + \frac{\Theta}{\gamma p_m}. \end{aligned} \tag{111}$$

From (103)

$$\|\mathbf{x}(t)\|^2 \leq \frac{p_M}{p_m} \frac{1}{\min_{\theta_f} \|\chi_k\|_1^2} \alpha^2 p_2^2 \mathbf{u}_{m_k}^2 \|\mathbf{x}(t_*)\|^2 + \frac{\Theta}{\gamma p_m}. \tag{112}$$

Finally, from the definition of $\mathbf{u}_s$

$$|\mathbf{u}_{s,k}(t)|^2 \leq \|\hat{\chi}_k(t)\|_1^2 \|\mathbf{x}(t)\|^2 \leq \max_{\theta_f} \|\chi_k\|_1^2 \|\mathbf{x}(t)\|^2. \tag{113}$$

From (112), (62), and the choices of γ in (86) and α in (60)

$$\begin{aligned} |\mathbf{u}_{s,k}(t)|^2 &\leq \frac{p_M}{p_m} \beta_k \alpha^2 p_2^2 \mathbf{u}_{m_k}^2 + \frac{\Theta \mu_k}{\gamma p_m} && (114) \\ &\leq p_2^2 \mathbf{u}_{m_k}^2. && (115) \end{aligned}$$

Thus, every kth component of the control signal stays inside the bounds

$$-p_2 \mathbf{u}_{m_k} \leq \mathbf{u}_{s,k} \leq p_2 \mathbf{u}_{m_k} \tag{116}$$

for all $t \geq t_*$ such that $\mathbf{u}_a(t) = \mathbf{u}_s(t)$. Therefore, it is guaranteed that on enforcing the control saturation condition for the adaptive case, the control signal stays within the specified limits.

VII. Numerical Examples

A. Purpose and Scope

Validation of the theoretical developments presented above is demonstrated in this section through simulation. The examples demonstrate the direction consistent mechanism for two unstable systems. The first example is a generic second-order plant. The tracking results are studied for two sinusoidal trajectories of different magnitudes. The purpose of this example is to simulate the response of the closed-loop system for two cases; one with tracking control within bounds and the other with tracking control outside control limits. Whenever the tracking control is within bounds, it is expected that the system demonstrates perfect tracking. Direction consistency is demonstrated for reference trajectories that require more control effort than that available.

The next simulation develops and evaluates control laws for a lateral/directional linear model representative of the F-16XL aircraft. This example demonstrates that the control laws developed earlier are also applicable to systems of the form

$$m\ddot{\mathbf{x}} + c\dot{\mathbf{x}} + k\mathbf{x} = 0. \tag{117}$$

This example presents the necessary equations for implementing control for kinematic tracking. The motive of this example is to compare the response of the system with and without the switching control law. It is demonstrated that without implementation of the switching control law the system goes unstable, while with the switching mechanism the plant state remains within bounds and consistent with the reference.

B. Second-Order Unstable Plant With Unknown Parameters

This example demonstrates the concept of a direction consistent constraint mechanism for an unstable second-order plant. The control objective is to restrict the states of the system to follow specified sinusoidal trajectories that are out-of-phase. The nominal plant used in the simulation is specified as

$$\bar{A} = \begin{bmatrix} 0.2 & 0.1 \\ 0.1 & -0.5 \end{bmatrix} \tag{118}$$

$$\bar{B} = \begin{bmatrix} 1 & 3 \\ -2 & 1 \end{bmatrix}. \tag{119}$$

The true plant matrices are randomly generated with an uncertainty of 5% in each element of $\bar{A}$ and $\bar{B}$ for the simulation. The control vector is symmetrically bounded between $[\pm 1 \quad \pm 1]^T$.

1) Case 1(a): The peak-to-peak amplitudes of reference for both the states is chosen to be 2. The frequency of oscillation for the specified reference is 1 rad/s and the two references are out-of-phase. λ is chosen as 0.2. The other design variables are $\alpha = 0.8856$, $s_1 = 0.97$, $s_2 = 0.98$, $p_1 = 0.985$, and $p_2 = 0.99$, with the adaptive gains chosen to be $\gamma = 1$, $\sigma_1 = 2$, and $\sigma_2 = 0.2$. The initial conditions of the system state is chosen as $x(0) = [0.02 \quad 0.02]^T$. Figs. 4 and 5 present results for this case. The plant state in this case perfectly follows the reference and $\mathbf{u}_{m_p}$ always remains less than unity. Moreover, since the tracking control computed using dynamic-inversion always remains within bounds, the applied control smoothly follows it. Further, the adaptive parameters are seen to remain within pre-computed bounds. Since the input is not sufficiently rich, the adaptive parameters shown in Fig. 5 do not converge to true values.

2) Case 1(b): In this case the peak amplitudes of the reference is increased to observe direction consistency. The amplitudes are chosen as $\mathbf{x}_{ref_1} = 1.5$ and $\mathbf{x}_{ref_2} = 2$ with same frequency of oscillations as in the previous case. Figs. 6 and 7 present the results. The plant state remains bounded and direction consistent with the desired reference when switching control is implemented. With the switching control law and direction consistent mechanism the applied control smoothly switches from tracking control to the saturated control and is direction consistent with the desired tracking control, without

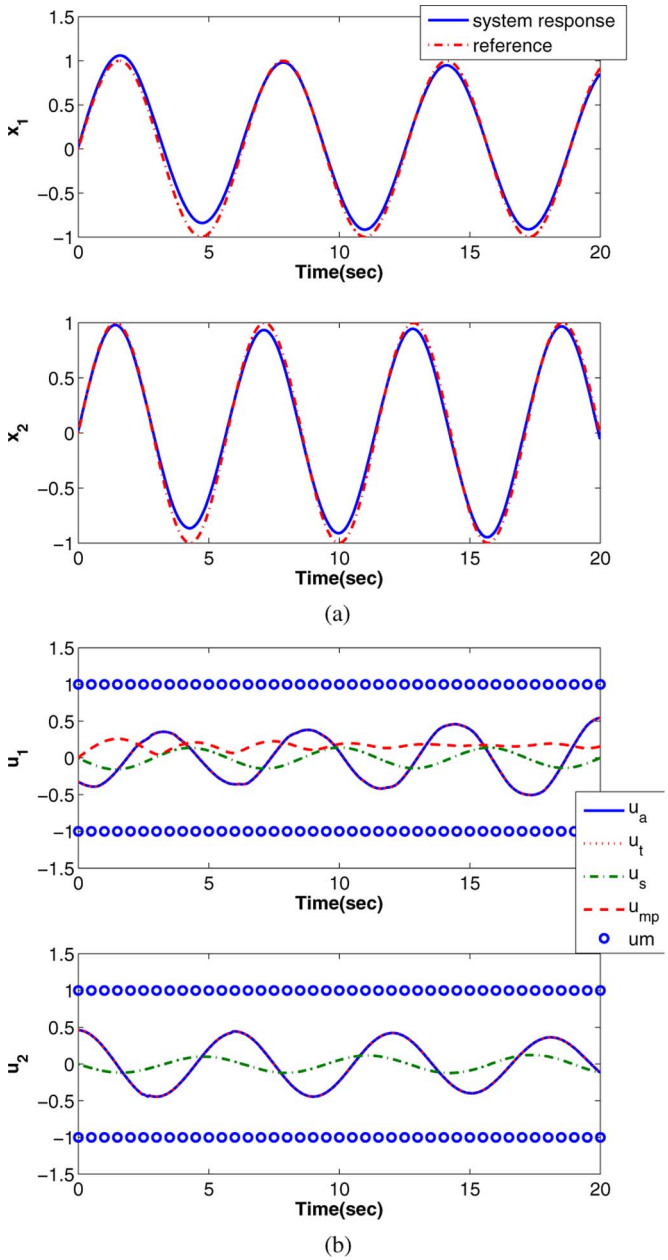

Fig. 4. Case 1(a) plant and control time histories. (a) Case 1(a): Plant State. (b) Case 1(a): Applied Control.

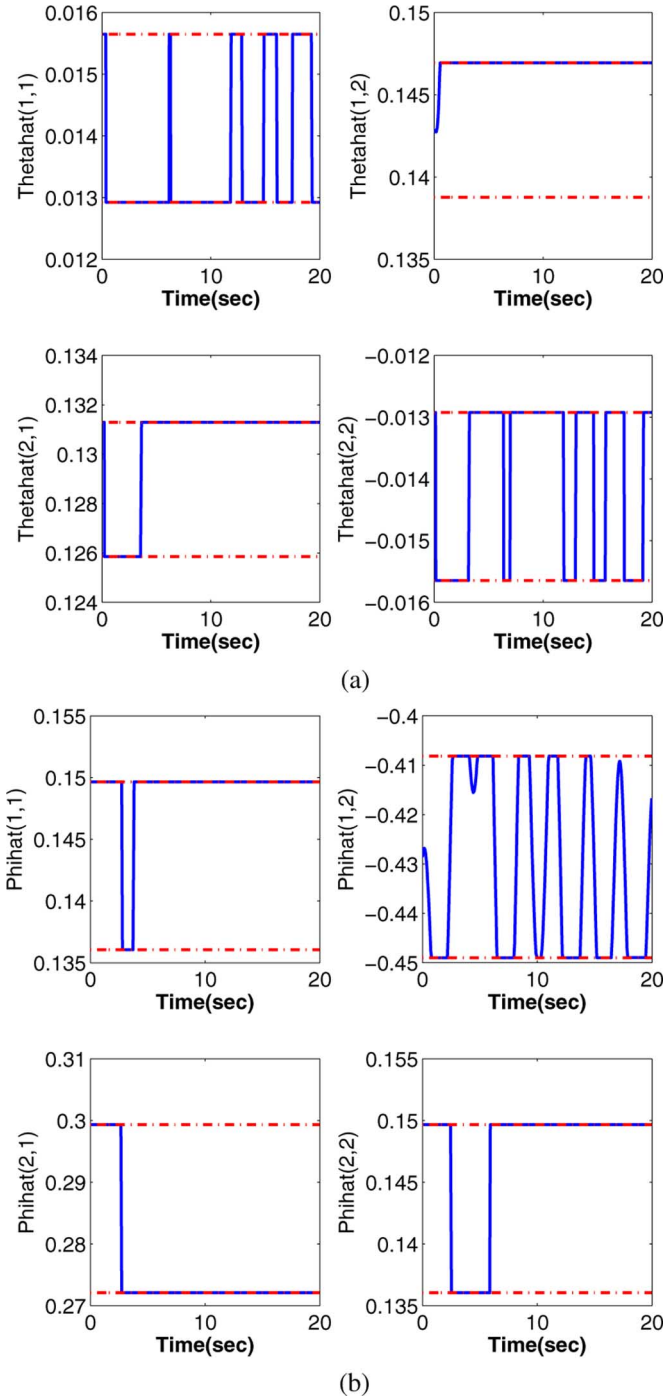

Fig. 5. Case 1(a): adaptive parameter time histories. (a) Case 1(a): Adaptive Parameter $\hat{\theta}$. (b) Case 1(a): Adaptive Parameter $\hat{\phi}$.

any control chattering as seen in Fig. 6(b). Also observe that since $\mathbf{u}_s$ remains within bounds, the ratio u_{mp} always remains less than 1.

Fig. 7 show the update of the adaptive parameters $\hat{\theta}$ and $\hat{\phi}$. The parameter projection successfully restricts the adaptive parameters within the parameter bounds. The adaptive parameters do not show any definite trend in the update. The important thing is to note that parameter convergence to a constant was demonstrated even in presence of errors due to control saturation.

C. F-16XL Aircraft

The objective is to command an aggressive maneuver which will saturate the controls. Using the F-16XL (see Fig. 8), the commanded maneuver is a bank angle doublet of $\pm$ 60 deg while simultaneously turning through a heading angle of -20 deg. The control effectors used here are aileron δ_{AA} and differential elevon δ_{EA}. While rudder is available as a control effector, it is not used here for the manueuver which constists primarily of rolling. The F-16XL linear model is displayed in the Appendix. All states and controls are perturbations from the steady, level, 1-g trimmed flight states given in Table I. The open-loop eigenvalues are $\lambda_{1,2} = -0.321 \pm 3.609j$, $\lambda_3 = -1.0138$, and $\lambda_4 = -0.032$.

1) Controller Synthesis: A reduced-order linear model is used to develop the controller. For the strictly lateral/directional

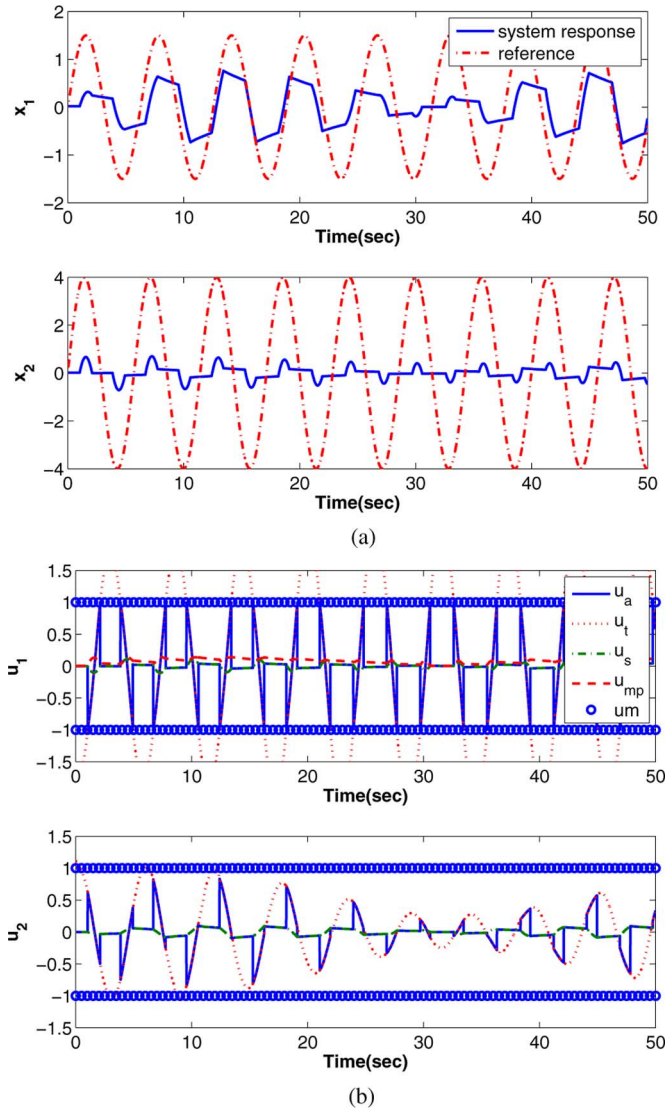

Fig. 6. Case 1(b) state and control time histories. (a) Case 1(b): Plant State. (b) Case 1(b): Computed Control.

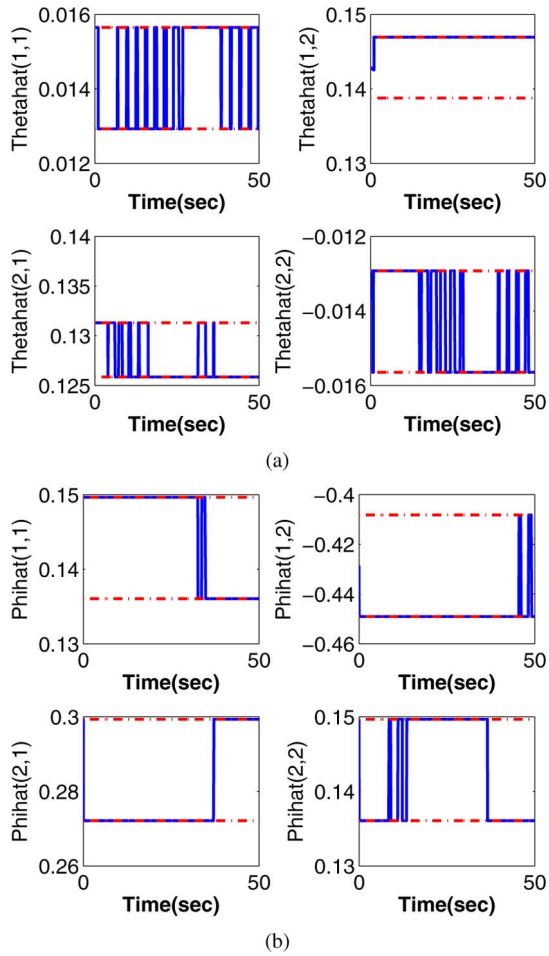

Fig. 7. Case 1(b) adaptive parameter time histories. (a) Case 1(b): Adaptive Parameter $\hat{\theta}$. (b) Case 1(b): Adaptive Parameter $\hat{\phi}$.

maneuver performed here, the longitudinal dynamics are neglected. The model is cast into a structured form as a kinematic part and a dynamic part using only the roll rate and yaw rate states. However, the full model is used for simulation.

Kinematic part

$$\dot{\phi} = p \tag{120}$$

$$\dot{\psi} = r. \tag{121}$$

Dynamic part

$$\begin{bmatrix} \dot{p} \\ \dot{r} \end{bmatrix} = \bar{A} \begin{bmatrix} p \\ r \end{bmatrix} + \bar{B} \begin{bmatrix} \delta_{AA} \\ \delta_{EA} \end{bmatrix} \tag{122}$$

where ϕ is the bank angle, ψ is the heading angle, and p and r are the roll and yaw rates, respectively. The control effectors are limited to maximum position limits of $\pm$ 25 deg. Uncertainty in the aircraft dynamical model is addressed by randomly introducing errors into the stability and control derivatives during numerical simulation. The reference trajectory is specified in terms of ϕ_r, ψ_r, p_r, r_r, $\dot{p}_r$, and $\dot{r}_r$. The control law and the update laws for the adaptive parameters are developed in accordance with the theory developed in the earlier sections. For

Fig. 8. F-16XL external physical characteristics.

TABLE I
TRIM STATE

Parameter	Value
Mach	0.90
Altitude	25,000 ft
Angle-of-Attack	4.61 degrees
Aileron δ_{AA}	0 degrees
Differential Elevon δ_{EA}	0 degrees

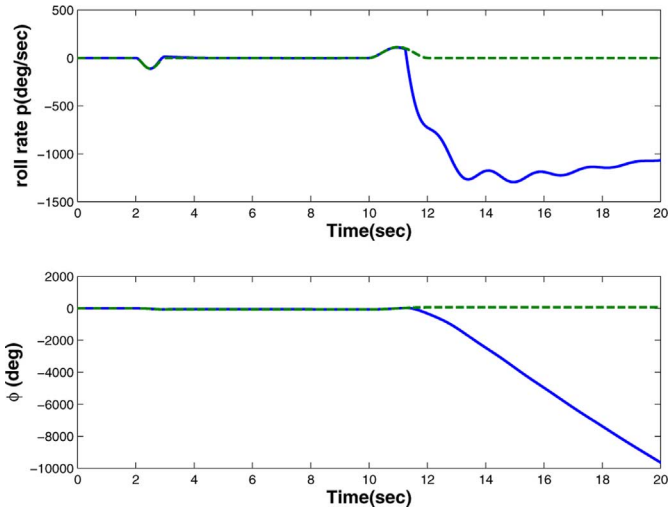

Fig. 9. Case 2(a) Roll rate and Bank Angle for F-16XL.

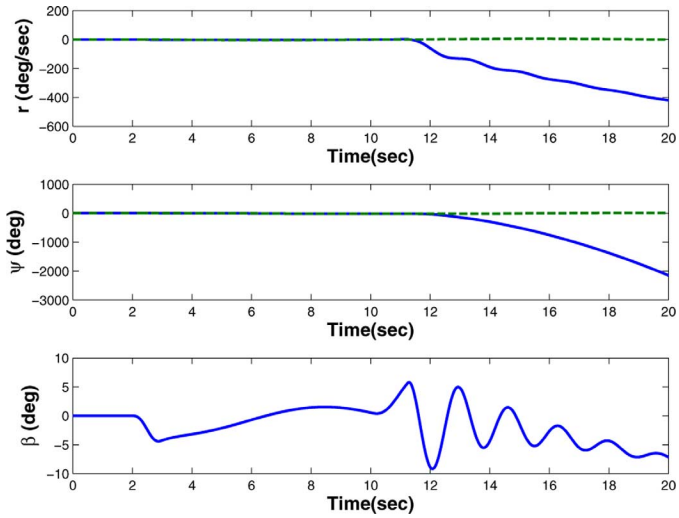

Fig. 10. Case 2(a) Yaw rate, heading angle, and sideslip angle for F-16XL.

brevity only the equations required for incorporating the control law in the simulation are presented here. The tracking errors are defined as

$$e_1 = \phi - \phi_r \tag{123}$$

$$e_2 = \psi - \psi_r. \tag{124}$$

To track the kinematic angles, the closed-loop dynamics are specified as

$$\begin{bmatrix} \dot{e_1} \\ \dot{e_2} \end{bmatrix} + \lambda \begin{bmatrix} e_1 \\ e_2 \end{bmatrix} + K_d \begin{bmatrix} e_1 \\ e_2 \end{bmatrix} = \mathbf{0}. \tag{125}$$

The design parameters are λ, K_d, γ, σ_1, σ_2, p_1, p_2, s_1, and s_2. The tracking and saturated control are

$$\mathbf{u}_t = -\hat{\theta} \begin{bmatrix} p \\ r \end{bmatrix} + \hat{\Phi}\vartheta \tag{126}$$

$$\mathbf{u}_s = -\hat{\theta} \begin{bmatrix} p \\ r \end{bmatrix} + (1 - u_{mp})\mathrm{Satdc}(\hat{\Phi}\vartheta) \tag{127}$$

where

$$\vartheta \triangleq \begin{bmatrix} \dot{p}_r + \lambda p_r - K_d e_1 \\ \dot{r}_r + \lambda r_r - K_d e_2 \end{bmatrix}. \tag{128}$$

The adaptive laws for the elements of $\hat{\theta}$ and $\hat{\Phi}$ are given by (84)–(85) with

$$\mathbf{e} = \begin{bmatrix} p - p_r \\ r - r_r \end{bmatrix} \tag{129}$$

and

$$\Lambda_x(\hat{\theta}_v - \theta_v) = (\hat{\theta} - \theta) \begin{bmatrix} p \\ r \end{bmatrix} \tag{130}$$

$$\Omega(\hat{\Phi}_v - \Phi_v) = (\hat{\Phi} - \Phi)\vartheta. \tag{131}$$

2) Results and Discussion: Case 2(a) No Switching Control Law For this case, once the control saturates maximum control is applied until the tracking control falls back into limits. Figs. 9–11 show that for the first 10 s the tracking control stays within bounds and the state is bounded. After 10 s, the tracking control required is large and the plant state diverges away from

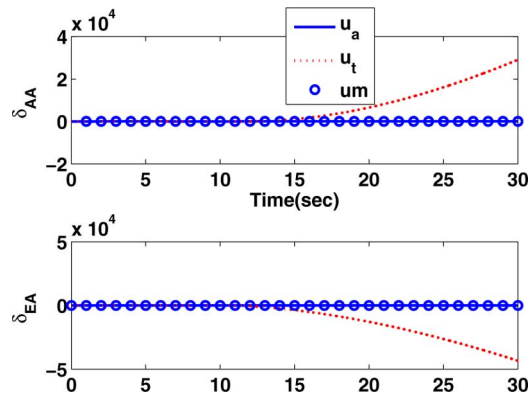

Fig. 11. Case 2(a) Aileron and Differntial Elevon for F-16XL.

the reference. Notice that without the switching control law the system becomes unstable.

Case 2(b) Switching Control Law In this case the switching control law is implemented. The design constants are chosen as $\gamma = 80$ which gives the value of $\alpha = 0.8582$, $\sigma_1 = 10$, $\sigma_2 = 10$, $s_1 = 0.9$, $s_2 = 0.92$, $p_1 = 0.96$, $p_2 = 0.98$, $\lambda = 10$, and $K_d = 10$. Figs. 12–16 present the simulation results. At 2 s the aircraft is commanded to roll at 112 deg/s to an angle of -60 deg and simultaneously turning to a heading of -20 deg at a yaw rate of 4.2 deg/s. Notice that the tracking control required to perform the maneuver is beyond the position limits specified, so the saturated control is applied since $u_{mp} = 0.9081$. This is greater than the specified s_1. The effect of applying this control is that the aircraft performs the roll at a reduced rate of 80 deg/s. At 2.7 s the tracking control lies within limits and the applied control stays there afterwards. The bank and heading angles settle down to their respective desired values at 10 s.

After 10 s the reference trajectory changes direction yet the system responds accordingly and starts to track closely. The aircraft is commanded to bank 60 deg at the rate of 110 deg/s, while simultaneously turning to 3.5 deg at a yaw rate of 5.4 deg/s. Since the tracking control is outside position limits, the saturated control is applied. As before the roll is performed at a reduced rate of 67.5 deg/s. The bank and heading angles settle to

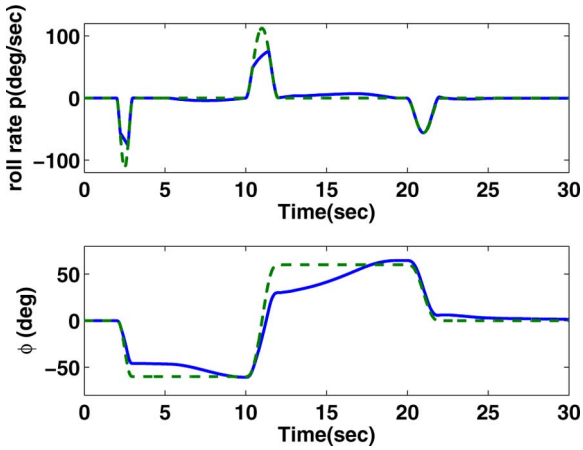

Fig. 12. Case 2(b) Roll rate and bank angle of F-16XL.

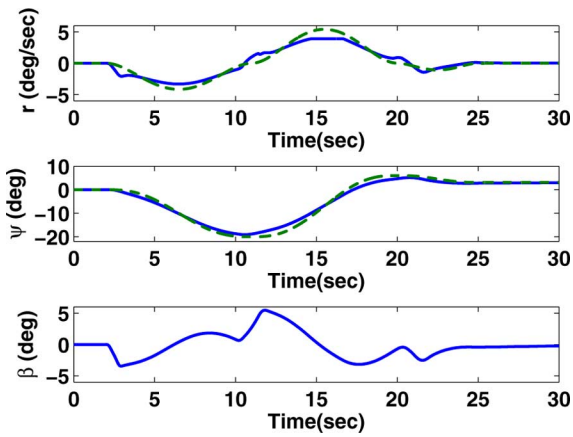

Fig. 13. Case 2(b) Yaw rate, heading, and sidelslip for F-16XL.

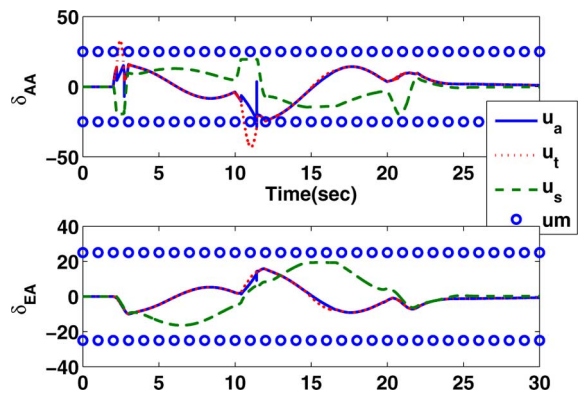

Fig. 14. Case 2(b) Aileron and differential elevon for F-16XL.

their respective values at 20 s, after which the aircraft is commanded to return to wings level, i.e., a 0 deg bank. This is commanded at a rate of 55 deg/s and the tracking control is applied within position limits. It is important to note that during this 30 s time span consistency with the reference is preserved, and control chattering is avoided. Even though sideslip angle β is not directly controlled, it remains within bounds and well behaved throughout the manuever. This is because the system is linear and minimum-phase so the internal dynamics are stable. Further, throughout the maneuver u_{mp} is maintained less than

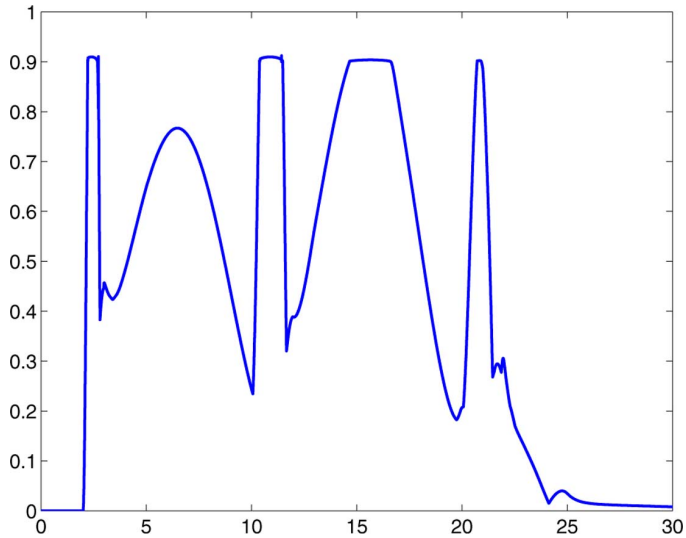

Fig. 15. Case 2(b) $\mathbf{u}_{mp}$ for F-16XL.

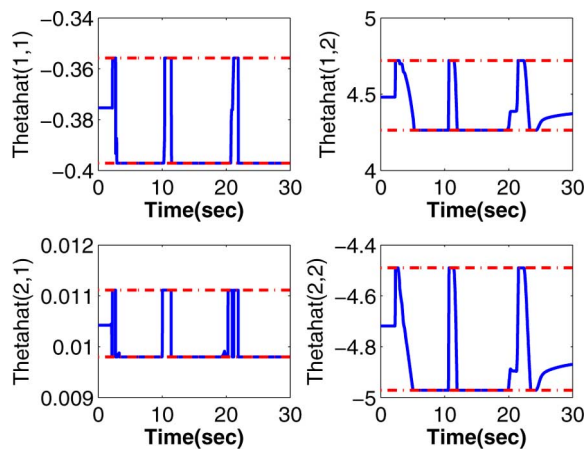

Fig. 16. Case 2(b) Adaptive parameters $\hat{\theta}$ for F-16XL.

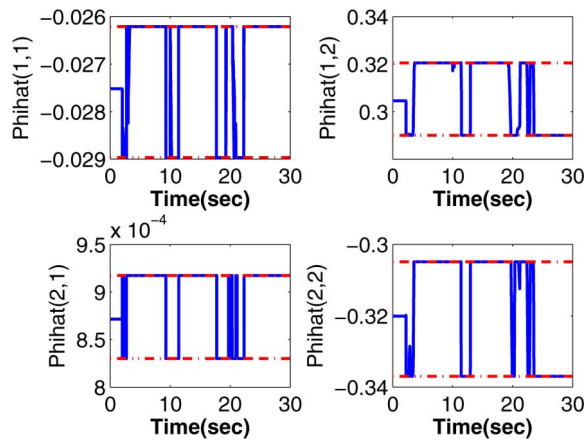

Fig. 17. Case 2(b) Adaptive parameter $\hat{\Phi}$ for F-16XL.

1. The adaptive parameters do not converge to their true values within the duration of the maneuver, because the reference trajectory is not persistently exciting. However, this is immaterial as asymptotic trajectory tracking can be achieved irrespective of parameter convergence.

VIII. Conclusion

Based on the stability proofs and the simulation results presented in the paper, if the control is unsaturated the tracking error asymptotically goes to zero, and all signals in the control scheme are bounded. If the control is saturated, the plant state can only be guaranteed to be bounded and direction consistent with the desired reference. The switching control strategy successfully restricts the state within the DCA. The transition between the tracking control and the stability control is smooth, and the applied control does not show any chattering. The instability protection switching control law can be implemented without prior explicit identification and bookkeeping of the DCA boundary. The control laws developed in this paper are applicable for unstable controllable linear time-invariant square non-singular systems with uncertainty within $\pm 5\%$ of the known nominal model.

Appendix

The F-16XL aircraft lateral/directional model

$$\begin{bmatrix} \dot{\beta} \\ \dot{p} \\ \dot{r} \\ \dot{\phi} \\ \dot{\psi} \end{bmatrix} = \begin{bmatrix} -0.128 & 0.0803 & -0.997 & 0.035 & 0 \\ -62.867 & -1.306 & 0.296 & 0 & 0 \\ 8.277 & 0.00472 & -0.259 & 0 & 0 \\ 0 & 1 & 0.0806 & 0 & 0 \\ 0 & 0 & 1 & 0 & 0 \end{bmatrix} \begin{bmatrix} \beta \\ p \\ r \\ \phi \\ \psi \end{bmatrix} + \begin{bmatrix} 0.00746 & 0.0344 \\ -37.467 & -35.645 \\ -0.102 & -3.221 \\ 0 & 0 \\ 0 & 0 \end{bmatrix} \begin{bmatrix} \delta_{AA} \\ \delta_{EA} \end{bmatrix}. \quad (132)$$

All angular quantities are in radians.

Acknowledgment

The authors would like to thank Dr. M. D. Tandale for insightful discussions and comments about this work.

References

[1] T. Hu and Z. Lin, *Control Systems with Actuator Saturation: Analysis and Design*, 1st ed. New York: Birkhauser (Springer), 2001.

[2] T. Hu, L. Qiu, and Z. Lin, "Controllability and stabilization of unstable lti systems with input saturation," in *Proc. IEEE Conf. Decision Control*, 1997, pp. 4498–4503.

[3] T. Hu, Z. Lin, and L. Qiu, "An explicit description of null controllable regions of linear systems with saturating actuators," *Syst. Control Lett.*, vol. 47, no. 1, pp. 65–78, Sep. 2002.

[4] D. Bernstein and A. A. Michel, "Chronological bibliography on saturating actuators," *Int. J. Robust Nonlinear Control*, vol. 5, pp. 375–380, 1995.

[5] S. P. Karason and A. M. Annaswamy, "Adaptive control in the presence of input constraints," *IEEE Trans. Autom. Control*, vol. 39, no. 11, pp. 2325–2330, Nov. 1994.

[6] M. R. Akella, J. L. Junkins, and R. D. Robinett, "Structured model reference adaptive control with actuator saturation limits," in *Proc. AIAA/AAS Astrodynam. Specialist Conf. Exhibit, Collection of Tech. Papers (A98-37348)*, 1998, pp. 10–13.

[7] E. N. Johnson and A. J. Calise, "Limited authority adaptive flight control for reusable launch vehicles," *J. Guid. Control Dyn.*, vol. 26, pp. 906–913, 2003.

[8] E. Lavretsky and N. Hovakimyan, "Positive μ-modification for stable adaptation in the presence of input constraints," in *Proc. Amer. Control Conf.*, 2004, pp. 2545–2550.

[9] D. Li, N. Howakimyan, and C. Cao, "$\mathcal{L}_1$ adaptive controller in the presence of input saturation," presented at the AIAA Guid., Nav., Control Conf. Exhibit, Chicago, IL, 2009.

[10] Y. Hong and B. Yao, "A globally stable high-performance adaptive robust control algorithm with input saturation for precision motion control of linear motor drive systems," *IEEE/ASME Trans. Mechatron.*, vol. 12, no. 2, pp. 198–207, 2007.

[11] N. E. Kahveci and P. A. Ioannou, "Indirect adaptive control for systems with input rate saturation," presented at the Amer. Control Conf., Seattle, WA, 2008.

[12] A. Leonessa, W. M. Haddad, T. Hayakawa, and Y. Morel, "Adaptive control for nonlinear uncertain systems with actuator amplitude and rate saturation constraints," *Int. J. Adapt. Control Signal Process.*, vol. 23, pp. 73–96, 2009.

[13] D. Enns, D. Bugajski, R. Hendrick, and G. Stein, "Dynamic inversion: An evolving methodology for flight control design," *Int. J. Control*, vol. 59, no. 1, pp. 71–91, Jan. 1994.

[14] J. Georgie and J. Valasek, "Evaluation of longitudinal desired dynamics for dynamic-inversion controlled generic reentry vehicles," *J. Guid., Control, Dyn.*, vol. 26, no. 5, pp. 811–819, Sep. 2003.

[15] D. Ito, D. T. Ward, and J. Valasek, "Robust dynamic inversion controller design and analysis for the x-38," presented at the AIAA Guid., Nav., Control Conf. Exhibit, Montreal, QC, Canada, 2001, AIAA-2001-4380.

[16] D. Ito, J. Georgie, J. Valasek, and D. T. Ward, "Re-entry vehicle flight control design guidelines, dynamic inversion," Final Tech. Rep., NASA TP-2002-210771, 2002.

[17] D. B. Doman and A. D. Ngo, "Dynamic inversion based adaptive/reconfigurable control of the x-33 on ascent," *J. Guid., Control, Dyn.*, vol. 25, no. 2, pp. 275–284, Mar. 2002.

[18] W. C. Durham, "Constrained control allocation," *J. Guid., Control, Dyn.*, vol. 16, no. 4, pp. 717–725, Jul. 1993.

[19] M. Tandale and J. Valasek, "Adaptive dynamic inversion control with actuator saturation constraints applied to tracking spacecraft maneuvers," *J. Astronaut. Sci.*, vol. 52, no. 4, pp. 517–530, 2005.

[20] P. J. Antsaklis and A. N. Michel, *A Linear Systems Primer*. New York: Birkhauser Boston, 2007.

[21] R. Bakker and A. Annaswamy, "Stability and robustness properties of a simple adaptive controller," *IEEE Trans. Autom. Control*, vol. 41, no. 9, pp. 1352–1358, Sep. 1996.

John Valasek (S'89–M'95–SM'98) received the B.S. degree in aerospace engineering from California State Polytechnic University, Pomona, in 1986 and the M.S. degree (with honors) and the Ph.D. degree in aerospace engineering from the University of Kansas, Lawrence, in 1991 and 1995, respectively.

From 1985 to 1988, he was a Flight Control Engineer with the Flight Controls Research Group, Aircraft Division, Northrop Corporation, where he worked on the AGM-137 Tri-Services Standoff Attack Missile (TSSAM) Program. He previously held an academic appointment with Western Michigan University during 1995–1997 and was a Summer Faculty Researcher with NASA Langley in 1996 and an AFOSR Summer Faculty Research Fellow with the Air Force Research Laboratory in 1997. Since then, he has been with the Department of Aerospace Engineering, Texas A&M University, College Station, where he is currently Professor of aerospace engineering and Director of the Vehicle Systems and Control Laboratory. He teaches courses on digital control, nonlinear systems, vehicle management systems, cockpit systems and displays, and flight mechanics. His current research interests include machine learning and multi-agent systems, intelligent autonomous control, vision-based navigation systems, and fault-tolerant adaptive control.

Prof. Valasek is a member of the Control Systems Society, the Systems, Man, and Cybernetics Society, the Computational Intelligence Society, and the Education Society. He was formerly an Associate Editor for dynamics and control of the IEEE Transactions on Education (1998–2001).

Maruthi Ram Akella is an Associate Professor with the Aerospace Engineering and Engineering Mechanics Department, The University of Texas at Austin. He has broad interests in dynamical systems and control theory for aero-mechanical systems. His theoretical contributions have found applications in astrodynamics and in the control of space systems and vision-guided robotics. His current research encompasses control theoretic studies of cooperating sensor and robotic agents accounting for measurement time-delays, kinematic constraints, and actuator saturations.

Prof. Akella is an Associate Fellow of the American Institute of Aeronautics and Astronautics (AIAA) and he currently serves as an Associate Editor for the IEEE TRANSACTIONS ON AEROSPACE AND ELECTRONIC SYSTEMS and the *Journal of Guidance, Control, and Dynamics*.

Anshu Siddarth (S'04) is originally from Hyderabad, India. She received the B.Tech. degree in electrical and electronics engineering (with honors) from Jawaharlal Nehru Technological University, Hyderabad, India, in 2006, and the Master of Science degree in aerospace engineering from the Indian Institute of Technology, Madras (IITM), India, in 2008. She is currently pursuing the Ph.D. degree from the Aerospace Engineering Department, Texas A&M University, College Station.

Her current research interests include adaptive control, nonlinear control and singularly perturbed systems.

Ms. Siddarth was a recipient of the "Academic Proficiency Award" in 2006, the "Tata Consultancy Services (TCS)-IITM" "best-in-class" fellowship in 2007, and the Amelia Earhart Fellowship for the 2011–2012 academic year.

Elizabeth Rollins (S'10) received the Magna Cum Laude with a B.S. degree in aerospace engineering from the University of Notre Dame, Notre Dame, IN, in 2007 and the S.M. degree in aeronautics and astronautics from Massachusetts Institute of Technology, Cambridge, in 2009. Currently, she is pursuing the Ph.D. degree in aerospace engineering from Texas A&M University, College Station.

She did research as a Draper Fellow at the Charles Stark Draper Laboratory during her time at MIT. As a member of the Vehicle Systems and Controls Laboratory, Texas A&M University, her current research focus is in the area of control theory and reinforcement learning.

Ms. Rollins was the recipient of an NSF Graduate Research Fellowship (2007). She is a member of Sigma Gamma Tau and Tau Beta Pi, and she was the recipient of the Sigma Gamma Tau Undergraduate Award in the Great Lakes Region (2007).